universität wien

MASTERARBEIT / MASTER'S THESIS

Titel der Masterarbeit / Title of the Master's Thesis

„Chemical and biological characterisation of novel rearrangement products of pirenzepine and derivatives“

verfasst von / submitted by

Lukas Skos, BSc

angestrebter akademischer Grad / in partial fulfilment of the requirements for the degree of

Master of Science (MSc)

Wien, 2020 / Vienna 2020

Studienkennzahl lt. Studienblatt / degree programme code as it appears on the student record sheet:	A 066 862
Studienrichtung lt. Studienblatt / degree programme as it appears on the student record sheet:	Masterstudium Chemie
Betreut von / Supervisor:	Assoz. Prof. Mag. Dr. Wolfgang Wadsak, Privatdoz.

Acknowledgments

Firstly, I would like to thank my supervisor Assoz. Prof. Mag. Dr. Wolfgang Wadsak, Privatdoz. for the opportunity to work at the Department of Medical Radiochemistry and Biomarker Development on a great topic in a rapidly growing and interesting scientific field.

I would like to especially convey my sincere gratitude to both of my co-supervisors Dr. Verena Pichler and Marius Ozenil, MSc. for their invaluable experience and advice throughout the whole thesis, for their constructive input and guidance shaping this work and their patience.

Furthermore, I would like to thank the Department of Pharmaceutical Chemistry of the University of Vienna, the hospital internal pharmacy of the Medical University of Vienna and Ing. Alexander Roller, Dipl.-Wirtschaftsing. (FH) from the X-ray Structure Analysis Centre of the University of Vienna for their contributions.

I would like to pay my special regards to the entire working group of the Division of Nuclear Medicine (Chrysoula, Eva, Karsten, Neydher, Sarah, Theresa, ...) for their warm welcome, helping me find my way around and everything non-work related as well as the working group of the Ludwig Boltzmann Institute for always answering my questions on subjects out of my field of study.

Also, I would like to say thank you to the students (Katharina, Julia, Anna and Tina) who worked alongside me during the time of this project for their unconditional help and the good times we spent.

Finally, I would like to express my deepest gratitude to my family and my girlfriend Tanja for their never-ending encouragement and whole-hearted support throughout my studies and this thesis.

Thank you all!

Zusammenfassung

Pirenzepin ist ein seit den 1970er Jahren zugelassener Wirkstoff aus der Gruppe der Parasympatholytika, der bei der Behandlung von Magengeschwüren zum Einsatz kommt. Pirenzepin wirkt als Antagonist für den M_1 Subtyp der muskarinischen Acetylcholinrezeptoren (mAChR), wodurch dieser gehemmt wird und die Ausschüttung der Magensäure verringert wird. Diese M_1 Subtyp Selektivität wird genutzt, um die Rezeptordichte und -verteilung in Gewebeproben zu erforschen. Bei der Evaluierung von neuartigen Liganden für die mAChR wurde ein literaturunbekanntes Umlagerungsprodukt entdeckt (unveröffentlichte Daten), das eine deutlich verminderte Bindungsaffinität zu diesen Rezeptoren aufweist. Ziel dieser Masterarbeit war es die Reaktionskinetik der Umlagerung genauer zu untersuchen, sowie die Auswirkungen auf physikochemische als auch biologische Eigenschaften zu bestimmen. Um festzustellen, ob die beobachtete Umlagerung auch bei strukturverwandten Wirkstoffen auftritt, wurden in diesem Projekt, neben Pirenzepin, zwei weitere Derivate (AFDX-384 und Telenzepin) in die Untersuchung miteinbezogen. Die literaturunbekannten Umlagerungsprodukte von Pirenzepin und Telenzepin konnten durch NMR, XRD und logP Messungen charakterisiert werden. Mittels neuentwickelter RP-HPLC-Methoden konnte die Umlagerungskinetik durch UV-Detektion verfolgt werden und zusätzlich gezeigt werden, dass die Umlagerungen quantitativ stattfinden. Die kinetischen Studien zeigten, dass eine Aktivierungsenergie von 83.2 ± 1.9 kJ/mol aufgebracht werden muss, um die Umlagerung von Pirenzepin einzuleiten. Durch die gesammelten Daten konnte ein Reaktionsmechanismus in Übereinstimmung mit den Ergebnissen der Kinetikmessung für eine saure Umlagerung aufgestellt werden. Weiters wurde die Stabilität von Pirenzepin in künstlicher Magensäure bestätigt, da auch nach 72 Stunden Reaktionszeit kein Umlagerungsprodukt nachgewiesen werden konnte. Im Zuge der Untersuchungen wurden auch neun kommerziell erhältliche Pirenzepin-Präparate von verschieden Anbietern auf deren Inhalt untersucht, wobei in zwei Präparaten das Umlagerungsprodukt nachgewiesen werden konnte. Daraufhin wurden die Hersteller der betroffenen Präparate auf die Verunreinigung aufmerksam gemacht. Um die biologische Aktivität der umgelagerten Wirkstoffe zu evaluieren, wurden in einem Brandel Harvester ein kompetitiver Radioliganden Assay mit der Filtrationsmethode durchgeführt, der zeigte, dass die Umlagerungsprodukte, im Vergleich zu deren Ausgangsstoffen, um drei Größenordnungen verminderten Affinitäten gegenüber allen fünf mAChR-Subtypen aufweisen. Folgeexperimente für diese Arbeit würden die Charakterisierung des AFDX-384 Umlagerungsprodukts beinhalten, sowie die allgemeine Bestimmung der potenziellen Einsatzmöglichkeiten der Umlagerungsstrukturen.

Abstract

Pirenzepine is a drug that is approved since the 1970s from the group of parasympatholytica for the treatment of gastric ulcers. Pirenzepine acts as an antagonist for the M_1 subtype of the muscarinic acetylcholine receptors (mAChR), thereby inhibiting the receptor and decreasing the secretion of gastric acid. This M_1 subtype selectivity can be utilized to determine the density and distribution of the receptor within tissue samples. During an evaluation of novel ligands for the mAChR a literature unknown structure had been discovered (unpublished results), which showed significantly different binding affinities towards those receptors. The aim of this master thesis was to closer investigate the chemical kinetics of the discovered rearrangement reaction as well as to identify the effects on the physicochemical and biological properties after the rearrangement. To determine if structurally similar active agents undergo an analogous rearrangement two derivatives (AFDX-384 and telenzepine) were included in this project. The literature unknown rearrangement products of pirenzepine and telenzepine were described through NMR, XRD and logP measurements. Firstly, with newly developed RP-HPLC gradient programs the rearrangement kinetics was monitored through UV-detection and additionally it was possible to show that the rearrangement occurred in a quantitative manner. The calculations of the kinetic studies presented that an activation energy of 83.2 ± 1.9 kJ/mol is necessary to initiate the rearrangement of pirenzepine. With the generated data it was possible to postulate a reaction mechanism for the rearrangement which is in agreement with the results of the kinetic measurements. Further, we could reaffirm the stability of pirenzepine in simulated gastric fluids where even after 72 hours reaction time no rearrangement product was detected. During the course of the examinations nine commercially available pirenzepine samples from different distributors were tested for their content whereby the rearrangement product was found in two samples. On base of this finding, producers were notified of the contamination in the respective samples. To determine the biological activity of the rearranged compounds competitive radioligand assays with the filtration method were conducted in a Brandel Harvester which exhibited a loss of three orders of magnitude in affinity towards all five mAChR subtypes compared to their respective starting materials. Follow-up experiments would include the characterisation of the AFDX-384 rearrangement product as well as the general determination of the potential field of application for the rearranged structures.

Table of contents

List of abbreviations

[^{3}H]NMS	[N-methyl-^{3}H] scopolamine methyl chloride
AChR	Acetylcholine receptor
BBB	Blood-brain barrier
cAMP	Cyclic adenosine monophosphate
CHO cells	Chinese hamster ovary cells
CNS	Central nervous system
EDQM	European directorate for quality of medicines and healthcare
EMA	European medicines agency
FDA	U.S. food and drug administration
IR	Infrared
LOD	Limit of detection
LOQ	Limit of quantification
mAChR	Muscarinic acetylcholine receptor
MS	Mass spectrometry
nAChR	Nicotinic acetylcholine receptor
NMR	Nuclear magnetic resonance
PET	Positron emission tomography
PLC	Phospholipase C
PNS	Peripheral nervous system
RL	Radioligand
RP-HPLC	Reverse phased-high performance liquid chromatograph
RT	Room temperature
SGF	Simulated gastric fluids

1 Introduction

1.1 Acetylcholine receptors (AChR)

The cholinergic system is part of the parasympathetic nervous system which is a subdivision of the autonomic nervous system that governs a wide range of subconscious bodily functions such as heart rate, blood pressure, respiration, arousal and digestion.[1,2] The main neurotransmitter in this system is acetylcholine and the cholinergic system comprises of two types of receptors, the nicotinic (nAChR) and muscarinic receptors (mAChR), which were named after the respective alkaloids binding specifically to the corresponding receptor type.[1–3] Both types of receptors can be found in the central nervous system (CNS) as well as the peripheral nervous system (PNS).[1–3] The nAChR are ligand-gated ion channels (fig. 1) comprising of five subunits (α, β, γ, δ and ε).[1–3] Depending on their location in the nervous system, the receptors are composed as homomers of just α subunits, as heteromers of α and β subunits or made up of four different subunits including the α subunits twice.[1–3] These receptors are considered to be the main interface for the interaction between nerves and muscles, but their responses also include release of further neurotransmitters.[1–3] Due to the nature of these functions, these responses are triggered and take effect rather quickly. In contrast, the mAChR are G protein-coupled receptors (fig. 1) with five distinctive subtypes which also regulate the release of neurotransmitters and are involved in cognitive tasks like memory and learning in the CNS and govern autonomous body functions in the PNS but operate more slowly.[1–3] Changes of the system mediated by the mAChR can take several seconds to few hours until implemented.[2]

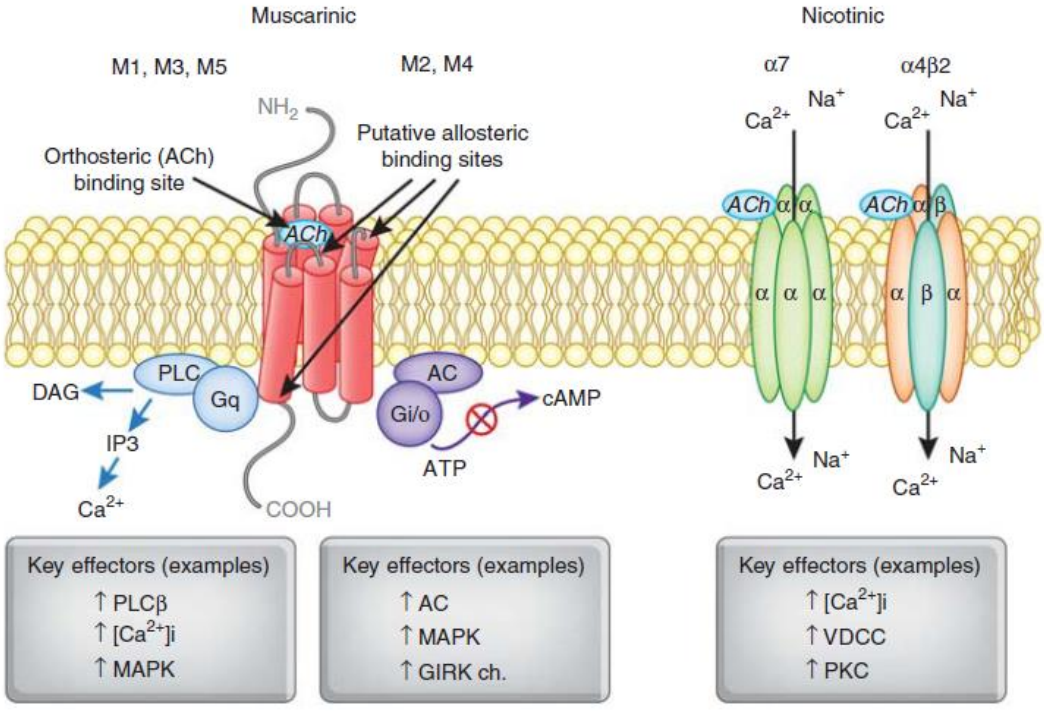

Figure 1: Schematic representation of the structure of mAChR and nAChR with their binding sites highlighted as well as subsequent signalling pathways (C. K. Jones, 2012).[3]

1.1.1 Muscarinic acetylcholine receptors (mAChR)

As mentioned in the previous chapter, the muscarinic acetylcholine receptors (mAChR) are part of the G protein-coupled receptor superfamily and are classified as A-type (rhodopsin-like) receptors, governing the signal transduction in the CNS, smooth muscles and certain target organs.[4–6] In the peripheral nervous system mAChRs process postganglionic stimuli which translate to changes in the parasympathetic nervous system and involuntary contractions of the heart and smooth muscles, whereas in the CNS mAChRs are found distributed throughout various regions of the brain with the M_1 subtype being the most prominent one, regulating cognitive functions and the release of other neurotransmitters.[4,5,7] Five subtypes (M_1 - M_5) have been identified through cloning of complementary DNA segments (CHRM1-5) encoding the respective subtypes.[4–7] Further, it could be shown that preferred combinations of mAChR subtypes with G proteins exist: M_1, M_3 and M_5 are typically coupled with a $G_{q/11}$-type protein and M_2 and M_4 are mostly associated with $G_{i/o}$-type protein.[4–7] The mAChR are transmembrane proteins consisting of seven alpha-helix domains with the recognition site embedded within the helices.[4–7] The G protein itself is a heterotrimer which constitutes of an α, β and γ subunit.[1,2,5] After a ligand is detected, conformational changes of the receptor complex transduce the signal into the cell to the coupled G protein.[5,6] If an odd numbered mAChR (M_1, M_3, M_5) is triggered the signal will initiate the phospholipase C (PLC) pathway. This pathway activates phospholipase C_β which induces the hydrolysis of phosphatidylinositol-4,5-bisphosphate to inositol trisphosphate and diacylglycerol which subsequently increases the Ca^{2+} concentration within the cytosol and activates protein kinase C.[1,4,5] In the case of the even numbered mAChR (M_2, M_4) the cAMP pathway will be induced which results in the inhibition of adenylyl cyclase or opening of potassium ion channels.[1,4,5] This leads to a decreased activity of cyclic adenosine monophosphate (cAMP)-dependant protein kinase A which regulates metabolic and transcriptional functions.[1,4,5] To date, the specific tasks of each receptor subtype could not be fully identified, but through studies with knockout mice certain effects could be assigned to each mAChR subtype, shown in table 1.[4,5,7]

Table 1: Associated functions of the mAChR subtypes identified through studies with knockout mice with the CHRM1-5 gene sequences respectively silenced (C. K. Jones et al., 2012; R. Aronstam and P. Patil, 2009; M. Ishii and Y. Kurachi, 2006).[3–5]

mAChR subtype	Location	Associated functions
M_1	Forebrain	Postsynaptic signal transduction, locomotion, learning, cognitive tasks
M_2	Smooth muscle and heart	Autoreceptor for ACh, involved in cognitive functions, analgesia, contractions of smooth muscle, body temperature, heart rate
M_3	Smooth muscle and glands	Contractions, salivation, body weight, urination, excretion
M_4	Midbrain, striatum and lung	Autoreceptor for ACh, potential innervation on the dopaminergic D_1 receptor, locomotion, release of dopamine and ACh
M_5	Only located in the substantia nigra and ventral tegmental area	Potential influence on dopaminergic system, dilatation of cerebral blood vessels

Muscarinic acetylcholine receptors are attractive drug targets for the treatment of a wide array of diseases. By addressing the peripheral mAChR it is possible to treat vastly different conditions such as peptic ulcers, incontinence and diabetes type 2.[4–6] In addition, symptoms of illnesses such as Alzheimer's, Parkinson's and schizophrenia can be alleviated due to the receptors close relation with the dopaminergic system in the CNS.[4,7] However, the homology among the recognition sites as well as the lack of deeper understanding is still holding back the potential of targeting the mAChR and designing subtype selective drugs or tracers is still a considerable challenge.[5–7]

1.2 Compounds of interest

The three substances investigated in this thesis (fig. 2; pirenzepine (**1**), AFDX-384 (**2**) and telenzepine (**3**)) are small molecule drugs with antagonistic effects towards the respective mAChRs and can be categorized as parasympatholytic compounds.

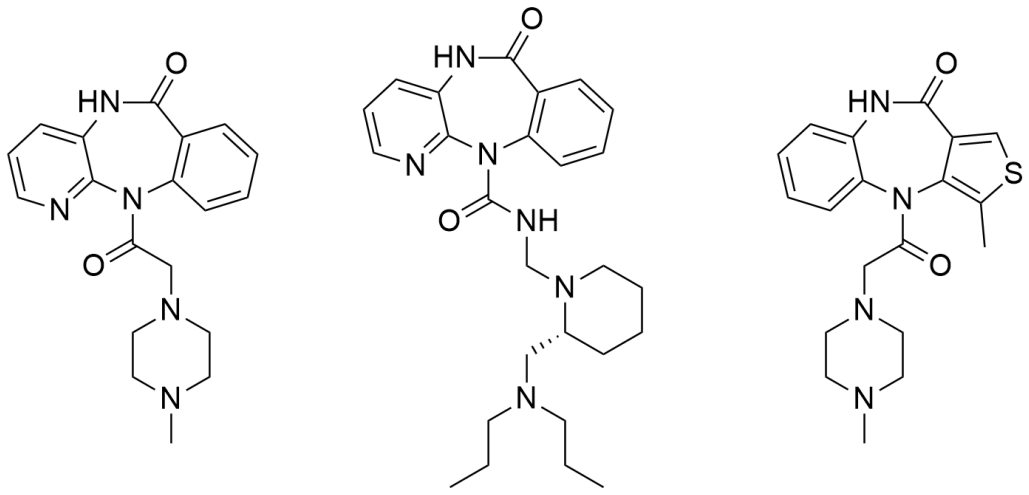

(**1**)	(**2**)	(**3**)
$C_{19}H_{21}N_5O_2$	$C_{27}H_{38}N_6O_2$	$C_{19}H_{22}N_4O_2S$
351.4 g/mol	478.6 g/mol	370.5 g/mol

*Figure 2: Structure, molecular formula and molecular weight of all three compounds under investigation. **1**: pirenzepine, **2**: AFDX-384, **3**: telenzepine.*

1.2.1 Pirenzepine

The drug pirenzepine (fig. 2, **1**) [11-[(4-methylpiperazin-1-yl)acetyl]-5,11-dihydro-6H-pyrido[2,3-b][1,4]benzodiazepin-6-one] is a tricyclic benzodiazepine with selective antagonism for the M_1 mAChR subtype.[8–13] It was developed in the 1970s and is approved by the European medicines agency (EMA) and the U.S. food and drug administration (FDA) to treat peptic and duodenal ulcers.[8–10,13] Pirenzepine is administered orally in the form of 50 mg tablets on an empty stomach and with a maximum dosage of 150 mg per day.[9,10] However, some years after its market launch pirenzepine got increasingly replaced by histamine H_2 receptor blockers and proton pump inhibitors which utilize a different mode of action to treat ulcers.[8] Nonetheless, the drug was successfully tested to postpone effects of myopia and is used in competitive binding studies of the M_1 mAChR.[9,12,14] The long record of administration of pirenzepine proves that it is generally well tolerated by patients.[9,12] Examinations have confirmed that the drug poorly permeates the blood-brain barrier (BBB) and does not induce any changes in the central nervous system or the composition of the serum.[9,10] Further, metabolization studies demonstrated that only a marginal amount of pirenzepine is metabolized and the resulting

desmethyl-pirenzepine does not show any biological activity.[9,10] The effects of pirenzepine are dose dependent.[9–11,13] The main targets are the peripheral M_1 mAChR which reduce the secretion of gastric acid, but with increasing amounts of the substance, additional subtypes of mAChR are addressed which cause anticholinergic adverse effects including dry mouth, blurred vision, headache, digestion problems and confusion.[8–10]

1.2.2 AFDX-384

The substance AFDX-384 (fig. 2, **2**) (N-(2-[(2R)-2-[(dipropylamino)methyl] piperidin-1-yl]ethyl)-6-oxo-5H-pyrido[2,3-b][1,4]benzodiazepine-11-carboxamide) is a selective M_2 and M_4 mAChR subtype antagonist which is primarily deployed as a tracer in autoradiography binding studies and is not approved as drug.[14–18] The structure of AFDX-384 (fig. 4) is analogous to pirenzepine as it only varies in the sidechain attached at the carbamate moiety. For a more thorough characterization of the compound Martin J. *et al*. investigated the stereochemical properties and found that in rat heart tissue the (R)-(-)-AFDX-384 isomer was 23 times more affine towards the mAChR than the (S)-(+)-enantiomer.[15] Another aspect examined in neuroimaging studies with AFDX-384 are the roles of the two mAChR subtypes in psychological disorders such as dementia, depression, schizophrenia and bipolar disorder.[14,16–18] Since AFDX does not penetrate the BBB sufficiently, it could not be used as a PET tracer for the mAChR in the CNS; however, it was suggested to be tested as a radioligand for cardiac imaging instead.[15,18]

1.2.3 Telenzepine

The compound telenzepine (fig. 2, **3**) (1-methyl-10-[2-(4-methylpiperazin-1-yl)acetyl]-5H-thieno[3,4-b][1,5]benzodiazepin-4-one) (fig. 5) is a derivative of pirenzepine and also acts as a selective M_1 antagonist.[19–23] It structurally differs from pirenzepine as its three-ring structure consist of a thienobenzodiazepine (fig. 5). Due to its chiral C-N bond (C_{Ph}-$N_{tert.}$) in the diazepine ring of the thienobenzodiazepine scaffold this compound has two isomers, (+) and (-), with a conversion rate of almost 1000 years at 20°C.[19,22] The (+)-isomer exhibits a 500 times higher activity of interacting with the mAChR than the (-)-isomer according to binding studies on cerebral cortex in rats.[22] This drug was developed to treat gastric ulcers.[19,20,22,24] However, it is not approved as a drug by the EMA. In regard of its antisecretory effect telenzepine shows a 4-10 times stronger response compared to pirenzepine and a four times higher affinity to the M_1 mAChR subtype.[20,21,24] By binding to the mAChR telenzepine inhibits subsequent stimuli in the peripheral system but it does not interfere with the mAChR in the CNS, since it does not penetrate the BBB.[20] Although telenzepine is not used in human treatment, the tritiated compound is utilized in competitive affinity studies for the mAChR based on its selectivity to the M_1 subtype.[19,21]

1.3 Chemical kinetic studies

Chemical reaction kinetics is a field of physical chemistry which examines the mechanism as well as parameters of a reaction such as temperature, time, presence of a catalyst and the starting concentrations.[25,26] The fundamental idea of chemical kinetics is that every reaction, however complicated it may be, can be broken down into basic mechanistic steps or a combination of these.[25,26] Therefore, a reaction mechanism has to be postulated which then is examined through spectroscopic monitoring of changes in the participating species concentration.[25,26] Afterwards, the obtained values are plotted and through fitting of the consequential function the kinetic parameters can be determined.[25,26] The yielded results are then compared with the hypothesized reaction mechanism and are examined if they are in an agreement.[25,26] These proposed reactions

can generally be formulated as differential equations called rate laws (eq. 1) with the solution of these characterizing the change of concentration over time:[25,26]

$$\frac{dx_i}{dt} = k_i[A]^a[B]^b \dots \quad (1)$$

Equation 1: General rate law which comprises of the concentration of the participating species in squared brackets, the reaction rate constant k_i describing the turnover of compounds over time and the exponents stemming from stoichiometric factors.

The reaction order is defined through the exponents in equation 1 with the sum of these expressing the total order of the reaction.[25,26] Further, the given order of the reaction does not have to correspond with the molecularity of the reaction which might indicate a more complex reaction mechanism.[25,26] The first category of reactions are first order reactions, general described in equation 2, with one molecule converting into one or more products:[25,26]

$$A \rightarrow B + C + \cdots \quad (2)$$

Equation 2: General representation of a first order reaction.

The rate law for the first order reaction is formulated as equation 3 and the solution of the differential equation is presented as equation 4:[25,26]

$$\frac{d[A]}{dt} = -k_1[A] \quad (3)$$

Equation 3: Rate law for first order reactions.

$$[A] = [A]_0 e^{-k_1 t} \quad (4)$$

Equation 4: Resolved rate law for first order reactions after integration.

A special case of first order reactions exists which is a bimolecular reaction where the change of concentration of one of the reaction partners appears to be constant over time due to being present in a vast surplus or acts as a catalyst.[25,26] This condition is called steady state.[25,26] Therefore, the rate law can be simplified to an equation where only the component which changes will be considered.[25,26] These reactions are called pseudo-first order reactions.[25,26] The second category are second order reactions with two molecules colliding and reacting to one or more products (eq. 5):[25,26]

$$A + B \rightarrow C + D + \cdots \quad (5)$$

Equation 5: General representation of a second order reaction.

These reactions are very common and in some cases two molecules of the same kind can react with each other (A + A).[25,26] The rate law with both reactants starting at the same concentration is given in equation 6 and its integrated form is shown in equation 7:[25,26]

$$\frac{d[A]}{dt} = -k_2[A]^2 \quad (6)$$

Equation 6: Rate law for second order reactions with both reactants starting at the same concentration.

$$\frac{1}{[A]} - \frac{1}{[A]_0} = -k_2 t \quad (7)$$

Equation 7: Resolved rate law for second order reactions after integration with both reactants starting at the same concentration.

There are two more categories of reaction order which can only come to pass under certain conditions. One being third order reactions, which require three molecules to collide simultaneously for the reaction to occur and thus hardly exist.[25] The other type are reactions with zeroth order kinetics where a steady state is achieved at the surface of a catalyst.[25,26] With these findings Arrhenius could derive, through empirical experimentation, the dependence of the reaction rate constant k_i on the temperature applied.[25–27] This led to the formulation of the Arrhenius equation:[25–27]

$$k_i = A * e^{\frac{-E_A}{RT}} \quad (8)$$

Equation 8: Arrhenius equation with A being the frequency factor, E_A the activation energy, R the ideal gas constant and T the absolute temperature.

When equation 8 is plotted in its logarithmized form with $\ln(k_i)$ vs the reciprocal absolute temperature the resulting linear function yields the activation energy divided through the ideal gas constant (E_A/R) and the logarihmized frequency factor ln(A).[25–27] Although generally valid, chemical reaction kinetics has limitations when it comes to its predictive capabilities. This is the case for reaction mechanisms involving many and complicated steps such as incomplete, consecutive reactions or reactions happening in parallel.[25] Additionally, due to the possibility of different reaction models resulting in the similar rate laws chemical kinetics is only capable to disprove or affirm a proposed reaction mechanism.[25]

1.4 Radioligand binding assays

Radioligand binding assays are an essential method to determine the interaction of two components with each other in biochemistry, cell biology, immunology and pharmacy.[28–30] Radioactively labelled ligands may be cytokines, hormones, neurotransmitters or drugs that interact with the receptor of interest.[28,30] In these studies it is possible to demonstrate how the chosen ligand influences a second messenger system, help to identify the receptors physiological function, show the distribution of the receptor in a tissue sample and help to categorize potential receptor subtypes.[30] Furthermore, if the tested compound is evaluated regarding its potential as a drug for the examined receptor, it should exhibit the following properties:[29]

- High affinity
- Low non-specific binding
- High specific activity
- Receptor specificity
- Potential to penetrate the blood-brain barrier
- Metabolization stability
- Low toxicity

The two parameters obtained from binding assays are on one hand the affinity of the ligand towards the receptor (K_D) and on the other hand the maximum density of the receptors (B_{max}).[29] The process of a ligand binding to a receptor is an intricate procedure which involves several different interactions such as H-bonds, ionic and van der Waals as well as changes in conformation.[29,30] Yet it is still possible to describe binding in a simplified mathematical model which is based on the law of mass action.[28,30] The assumptions for this model are (a) that the binding is reversable, (b) the components do not change during the binding process, (c) all

components are equally available and (d) there is only a bound and a free state.[30] Therefore, this model can be considered valid for all reversible bimolecular reactions which are at equilibrium (eq. 9):[28]

$$A + B \leftrightarrows AB \tag{9}$$

Equation 9: General chemical equation for a reversible bimolecular reaction.

The chemical reaction (eq. 9) can be also formulated as equation 10 where the left side describes the formation of the product (AB) with a second order reaction rate constant (k_{on}) and the right side describes the dissociation with a first order reaction rate constant (k_{off}).[28]

$$k_{on} * [A][B] = k_{off} * [AB] \tag{10}$$

Equation 10: Equation describing the equilibrium through the association and dissociation of the components.

With the rearrangement of equation 10 the equilibrium constant (K_{eq}) is obtained with the unit of M^{-1} (eq. 11):[28,30]

$$K_{eq} = \frac{k_{on}}{k_{off}} = \frac{[AB]}{[A][B]} \tag{11}$$

Equation 11: Definition of the equilibrium constant (K_{eq}) through the law of mass action.

Finally, for the description of the affinity of the ligand towards the receptor the reciprocal of the equation constant is formed which gives the dissociation constant (K_D) with the unit M (eq. 12).[28]

$$K_D = \frac{k_{off}}{k_{on}} = \frac{[A][B]}{[AB]} \tag{12}$$

Equation 12: Reciprocal of the equilibrium constant (K_{eq}) characterizing the dissociation constant (K_D).

The definition of K_D being a reciprocal value, means that the lower the number the stronger the affinity of the ligand becomes and the more the balance is shifted towards the product side of the equation.[28] If K_D is unknown it can be determined through saturation binding experiments which measure specific binding.[29,30] In this format a set amount of receptor is brought *in vitro* to equilibrium with increasing concentrations of radioligand under constant conditions.[29] Then, the equilibrium will be disrupted by removing all free ligand and measuring the remaining radioactivity bound to the receptor.[29] The yielded values are analysed in a Scatchard plot (fig. 3).[29] In this display the ratio of bound and free ligand (B/F) is plotted against the bound radioligand (B).[29] The slope of the resulting linear function represents the negative reciprocal K_D and the intercept with the x-axis stands for the estimated maximum density of the receptors (B_{max}).[29] The shape of the graph of the Scatchard plot can also appear in a concave form if the ligand exhibits different affinities towards present subtypes of the receptor.[29,30] By setting the measured B_{max} in relation to a standardized reference, this value can be compared with samples originating from different tissue or across different studies.[29]

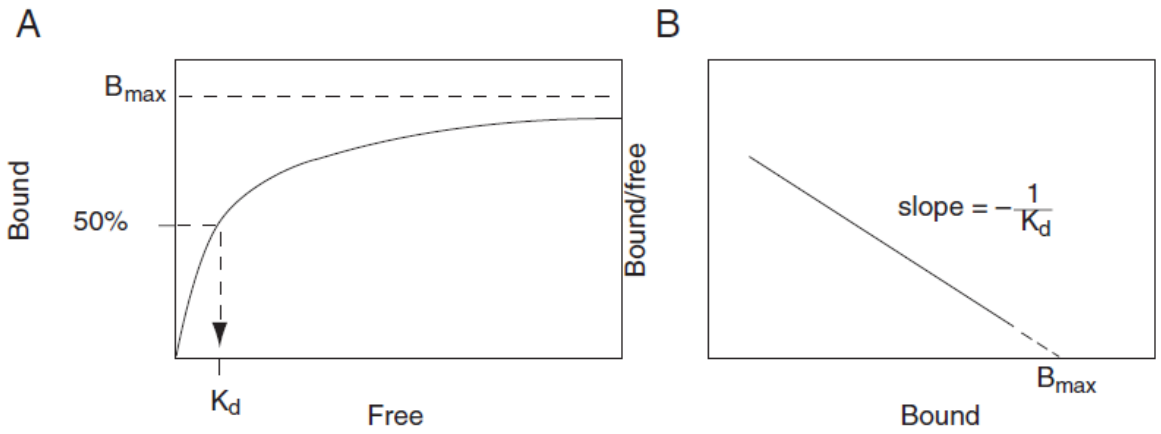

Figure 3: Representative graphs for saturation binding experiments. A: saturation binding experiment determining the amount of specific binding and B: exemplary Scatchard plot obtained through transforming data from graph A. (H. Motulsky and R. Neubig, 2002)[30]

With the newly measured or known K_D, competitive binding experiments can now be conducted which will yield the IC_{50} value, which is the concentration of the unlabelled compound blocking half the specific binding sites (fig. 4).[29] Additionally, this method allows for determining the selectivity of the substance of interest towards receptor subtypes.[29] The method for measuring this parameter is to displace a constant amount of radioligand by a varying amount of unlabelled competitor.[29] Similarly, for the saturation binding experiments, all components are brought to equilibrium under constant conditions, unbound components will be washed away, and the remaining activity is measured.[30]

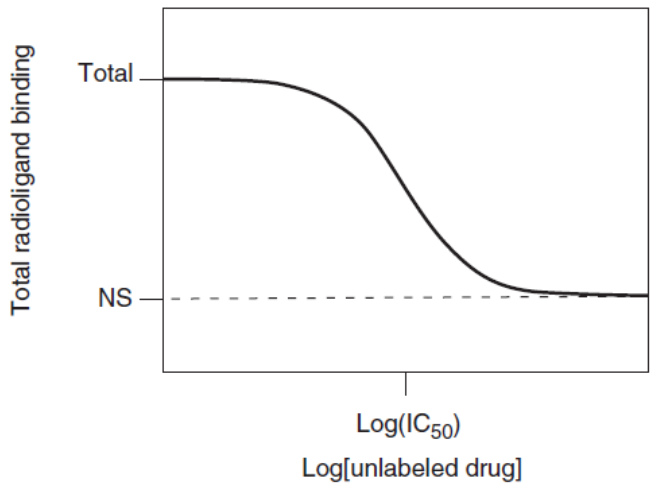

Figure 4: Representative sigmoid curve of a competitive binding assay. (H. Motulsky and R. Neubig, 2002)[30]

However, the experimental conditions chosen, such as temperature, chosen buffer and concentration range, can have a great impact on the result of the IC_{50} value.[30,31] Therefore, the inhibition constant (K_i), which is independent of the experimental setup, is commonly used for better comparability.[30,31] K_i is then calculated through the Cheng-Prussoff equation (eq. 13) which establishes a relation between the inhibition constant and the IC_{50} value:[30,31]

$$K_i = \frac{IC_{50}}{1 + \frac{[RL]}{K_D}} \tag{13}$$

Equation 13: Cheng-Prusoff equation with Ki being the inhibition constant describing the affinity of the unlabelled compound towards the receptor and [RL] stands for the used concentration of radioligand.

As mentioned at the beginning of this chapter this binding model is just an approximation and is limited in its potential to show the real affinity, since experiments are conducted under non-physiological conditions and effects like metabolization are not accounted for.[32]

2 Aim

The goal of this master thesis was to investigate a preliminarily observed rearrangement reaction of pirenzepine and structural congeners yielding literature-unknown substances. The rearrangement reaction of pirenzepine and its derivatives AFDX-384 and telenzepine were examined by RP-HPLC to determine reaction conditions and kinetic values. Moreover, the rearrangement reaction was performed in simulated gastric fluids under physiological conditions due to pirenzepine's oral administration and the potential, unwanted formation of the side product *in vivo*. Commercially available pirenzepine samples from different suppliers were examined for their content of the rearrangement product, as this unwanted product was found in commercially available products falsely labelled as being pirenzepine. The novel isolated rearrangement products were fully characterized by UV-detection, NMR and XRD. Moreover, their physicochemical parameters, like logP value and stability, were assessed in comparison to their non-rearranged counterpart. Finally, all identified rearrangement products were evaluated in regard to their affinities towards all mAChR subtypes *via* a competitive displacement assay in a Brandel Harvester.

3 Materials

3.1 Chemicals

- Acetone (*Sigma Aldrich*)
- Acetonitrile (ACN, HPLC grade, *Sigma Aldrich*)
- AFDX-384 (*Tocris Bioscience*)
- Ammonium dihydrogen phosphate (*Sigma Aldrich*)
- Ammonium dihydrogen phosphate buffer (25 mM, pH 9.3 adjusted with NaOH)
- Chloroform (*Merck*)
- Dichloromethane (DCM, *Merck*)
- Dimethyl sulfoxide (DMSO, *Sigma Aldrich*)
- Ethylenediaminetetraacetic acid (EDTA, *Sigma Aldrich*)
- Ethanol (EtOH, 96% Eu. Phr., *Merck*)
- Ethyl acetate (*Merck*)
- Foetal bovine serum (FBS, *Gibco*)
- Gastrozepin® (Pirenzepine, *Boehringer Ingelheim*)
- Geneticin (G418, *Gibco*)
- Ham's F12 Nutrient Mix (*Gibco*)
- Hydrochloric acid (HCl, 36%, *VWR Chemicals*)
- L-Glutamine (*Gibco*)
- Methanol (MeOH, *Merck*)
- Magnesium chloride ($MgCl_2$, *Merck*)
- n-Hexane (*Sigma Aldrich*)
- [N-methyl-^{3}H] scopolamine methyl chloride ([^{3}H]NMS, 37 MBq, 2.964 TBq/mmol in 1 mL ethanol, *Perkin Elmer*)
- Pepsin (from porcine gastric mucosa, 3200-4500 units/mg protein, *Sigma Aldrich*)
- Phosphate-buffered saline (PBS, *Gibco*)
- Phosphate-buffered saline (PBS, 10-fold concentrated, *Morphisto*)
- Phosphoric acid (85%, *Merck*)
- Polyethyleneimine (PEI, 50% in water, *Fluka Analytical*)
- Protease inhibitor cocktail powder P2714 (content of a vial dissolved in 10 mL purified water for a 10-fold concentrated solution and aliquoted as 200 µL units, stored at -20°C; composition:
    - 2 mM M 4-(2-aminoethyl) benzenesulfonyl fluoride
    - 1 mM EDTA
    - 130 µM bestatin
    - 14 µM E-64
    - 1 µM leupeptin
    - 0.3 µM aprotinin) (*Sigma Aldrich*)[33,34]
- Scopolamine hydrobromide (*Sigma Aldrich*)
- Sodium chloride (NaCl, Bioreagent, *Sigma Aldrich*)
- Sodium hydrogen carbonate (*Merck*)
- Sodium hydroxide (NaOH, 1M, *Merck*)
- Sodium phosphate dibasic dehydrate (*Sigma Aldrich*)
- Sodium phosphate monobasic monohydrate (*Sigma Aldrich*)
- Sulfuric acid (H_2SO_4, 95-97%, *Merck*)

- Telenzepine dihydrochloride hydrate (*Sigma Aldrich)*
- Tetrahydrofuran (THF, *Merck*)
- Toluene (*Merck*)
- Tris(hydroxymethyl)aminomethane **(**Tris, *Merck*)
- Trypsin (0.05%, *Gibco*)
- Ultima Gold™ scintillation cocktail (*Perkin Elmer*)

3.2 Equipment

- Brandel 36 channel harvester with GF/B filter
- Hidex 300SL
- HPLC setup:
    - Agilent 1200 series quaternary pump and degasser
    - Agilent 1100 series UV detector (upgraded to G1315B DAD) and autosampler
    - Columns:
        - XSelect HSS T3 (3.5 µm, 100 x 4.6 mm)
        - apHERA (5 µm, 10 x 6 mm)
- Sorvall ultracentrifuge combi OTD

3.3 Software

- Gina Star 5.9 + Service Pack 17
- GraphPad Prism 6
- Microsoft office package 2016
- MikroWin 200 4.44
- Olex^2 1.2.10

4 Methods

4.1 Rearrangement reaction and HPLC analysis

The initial characterization of the compounds of interest was conducted through a HPLC setup with UV-detection (sec. 3.2) at 216 nm and 254 nm and a flow rate of 1 mL/min with a XSelect HSS T3 column (3.5 µm, 100 x 4.6 mm) at RT. Starting from an already developed method, which effectively separated pirenzepine from its rearrangement product, an individual program for each derivative was established. Beforehand a basic 25 mM $(NH_4)H_2PO_4$ buffer (pH 9.3) and 100 µg/mL solutions of the test substances, 12 M, 1 M and 0.2 M HCl solutions as well as a $NaHCO_3$ quenching solution (55.55 mg/mL) were prepared. Pirenzepine and telenzepine were used as aqueous solutions, whereas AFDX-384 was dissolved in EtOH due to its low solubility in water.[35] Rearrangement products were prepared by reacting 50 µL of pirenzepine (100 µg/mL in H_2O), telenzepine (100 µg/mL in H_2O) or AFDX (100 µg/mL in EtOH) with 50 µL aqueous HCl (0.2 M - 12 M) in agitated polypropylene reaction tubes. After the respective reaction time of the mixtures of HCl and compound solution, a 5 µL sample was carefully quenched with 45 µL $NaHCO_3$ solution in a glass inlay of the HPLC vials. For measurements 20 µL of the sample solutions were injected onto the column. After thorough testing, the final gradient programs were built from a combination of acetonitrile (ACN), the basic 25 mM $(NH_4)H_2PO_4$ buffer (pH 9.3) and purified water in different proportions for the respective compound.

4.1.1 Statistics

All HPLC experiments were conducted in at least three repetitions and calculations were performed in MS Excel if not stated otherwise.

4.1.2 Pirenzepine

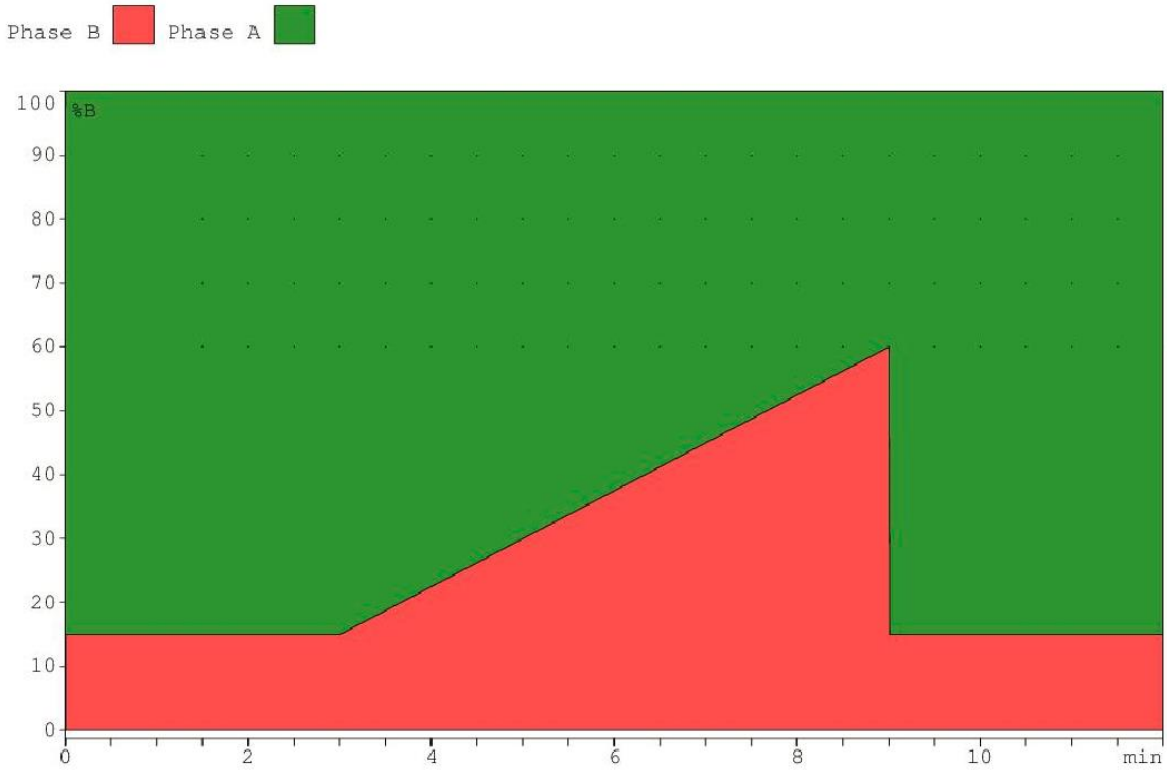

Figure 5: Gradient method for the analysis of pirenzepine and its rearrangement product with a run time of 12 minutes and equilibration phase of three minutes before each run (not included in graph). Phase A (green) is the 25 mM $(NH_4)H_2PO_4$ buffer (pH 9.3) and phase B (red) is acetonitrile (ACN).

Table 2: Timetable and percentages of used solvents for the pirenzepine separation method.

Time [min]	A: 25 mM $(NH_4)H_2PO_4$ buffer (pH 9.3) [%]	B: ACN [%]	C: Water [%]
Initial	85	15	-
3	85	15	-
9	40	60	-
9.01	85	15	-

The final gradient program for pirenzepine consisted of a total run time of 12 minutes per measurement and an additional equilibration phase of three minutes (not included in the figure 5) before the HPLC program started (fig. 5 and tab. 2). In the first three minutes of the measurement the elution was kept isocratic and then the percentage of organic phase was increased to shorten the retention time of pirenzepine.

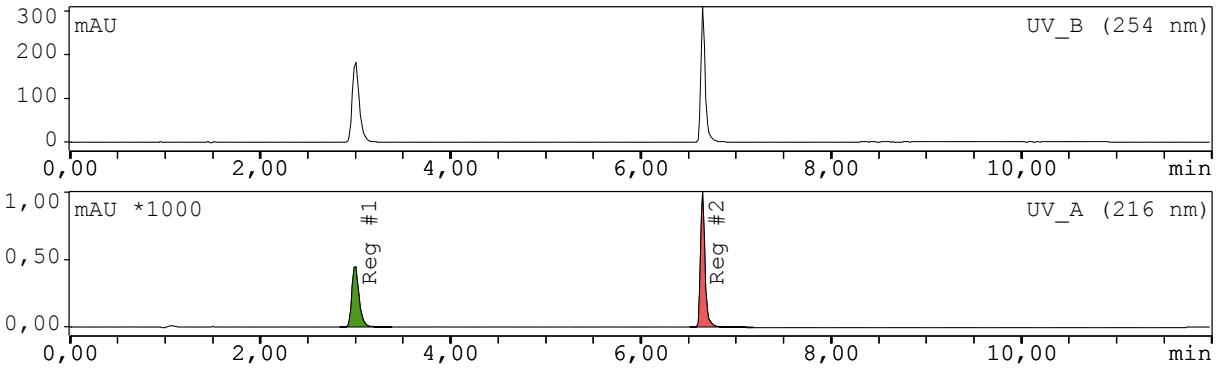

Figure 6: Representative HPLC chromatogram for a mixture of pirenzepine and its rearrangement product (sec. 4.1.5) with UV-detection at 254 nm (above) and 216 nm (below). The rearrangement product appears at 3.01 min and pirenzepine at 6.66 min. Dead time was 1.15 min.

The pirenzepine method lead to retention times of pirenzepine at 6.66 min, the rearrangement product at 3.01 min and the dead time at 1.15 min (fig. 6). Retention factor (k') for pirenzepine is 4.8 and 1.6 for its rearrangement product.

4.1.3 AFDX-384

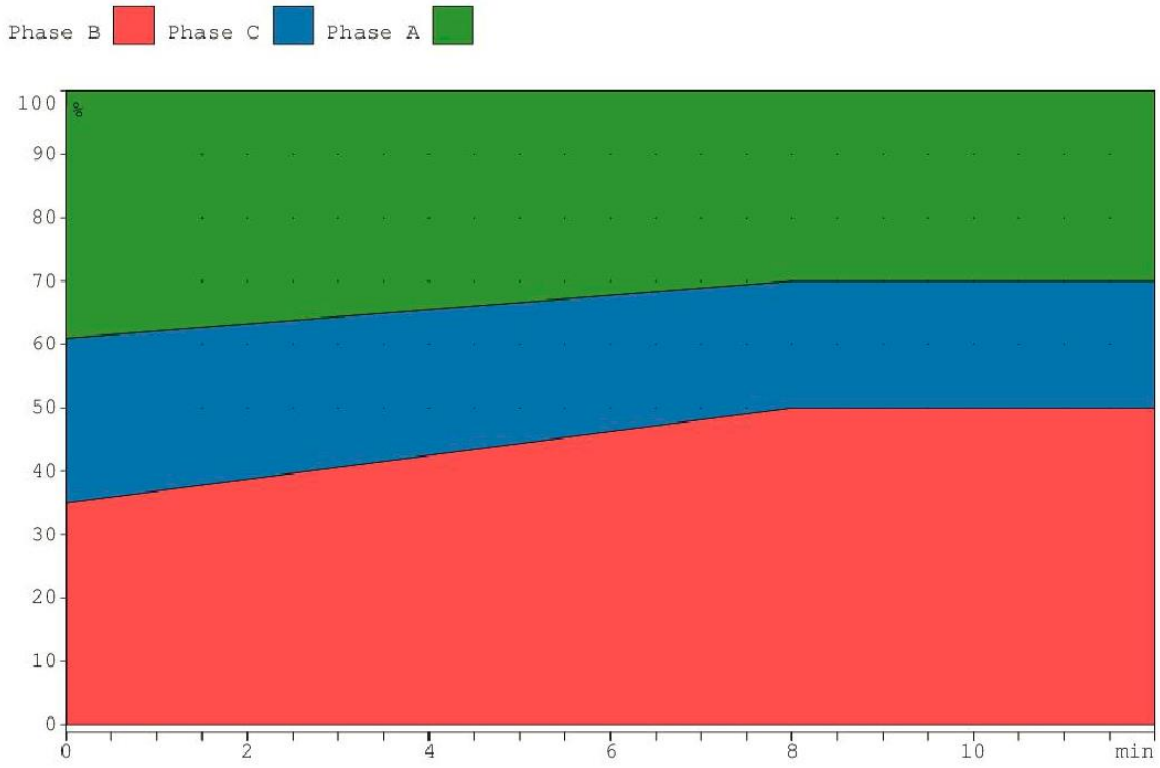

Figure 7: Gradient method for the analysis of AFDX-384 and its potential rearrangement product with a run time of 12 minutes and equilibration phase of three minutes before each run (not included in graph). Phase A (green) is the 25 mM $(NH_4)H_2PO_4$ buffer (pH 9.3), phase B (red) is ACN and phase C (blue) is purified water.

Table 3: Timetable and percentages of used solvents for the AFDX-384 separation method.

Time [min]	A: 25 mM $(NH_4)H_2PO_4$ buffer (pH 9.3) [%]	B: ACN [%]	C: Water [%]
Initial	39	35	26
8	30	50	20

The developed method for the separation of AFDX-384 and potential rearrangement product consisted of a gradient using the basic $(NH_4)H_2PO_4$ buffer, ACN, and water (fig. 7 and tab. 3) with a run time of 12 minutes and an equilibration phase before the program of three minutes (not included in the figure 7). In this separation program water was added in order to dilute the buffer concentration to improve the separation.

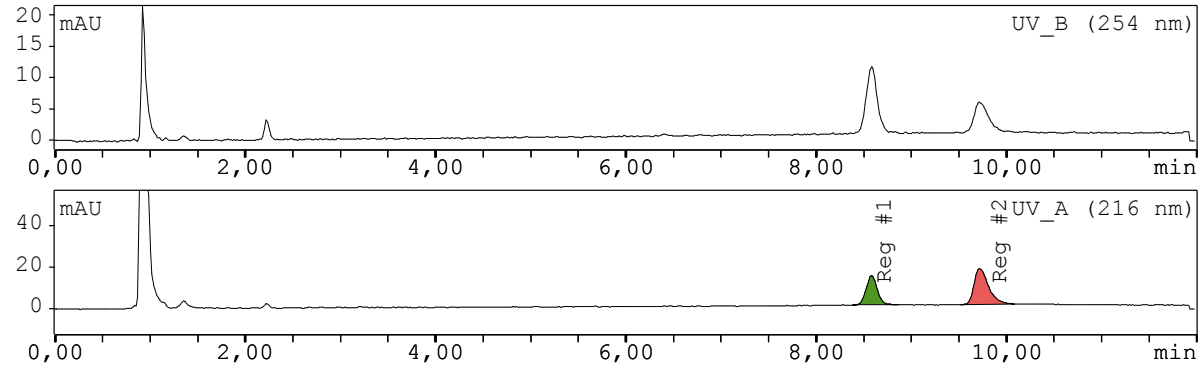

Figure 8: Representative HPLC chromatogram of AFDX-384 after 1 hour at 75°C with 0.5 M HCl and UV-detection at 254 nm (above) and 216 nm (below). The rearrangement product appears at 8.59 min and AFDX-384 at 9.73 min. Dead time was 0.98 min.

The AFDX-384 separation program yielded retention times of 9.73 min for the starting compound, 8.59 min for its potential product and a dead time of 0.98 min (fig. 8). The k'-value for AFDX-384 is 8.9 and 7.8 for the rearrangement product.

4.1.4 Telenzepine

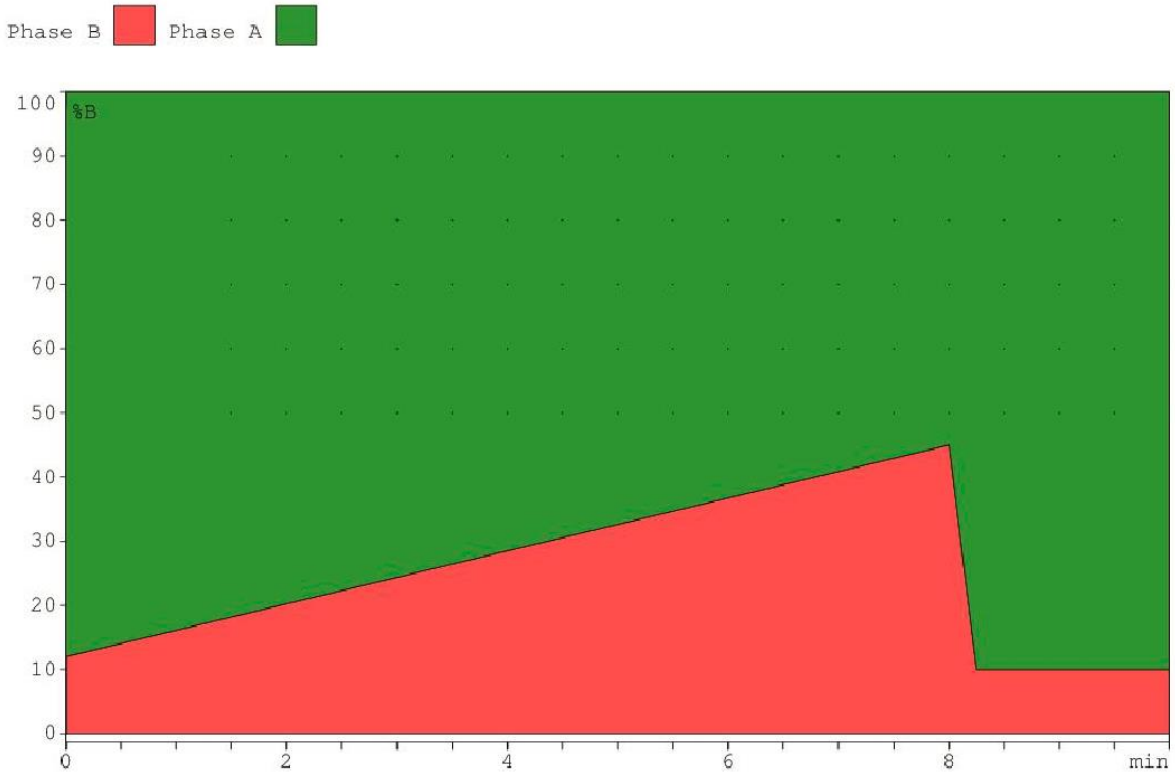

Figure 9: Gradient method for the analysis of telenzepine and its rearrangement product with a run time of 10 minutes and equilibration phase of two minutes before each run (not included in graph). Phase A (green) is the 25 mM $(NH_4)H_2PO_4$ buffer (pH 9.3) and phase B (red) is ACN.

Table 4: Timetable and percentages of used solvents for the telenzepine separation method.

Time [min]	A: 25 mM $(NH_4)H_2PO_4$ buffer (pH 9.3) [%]	B: ACN [%]	C: Water [%]
Initial	88	12	-
8	55	45	-
8.25	90	10	-

Telenzepine was measured with a gradient program as depicted in figure 9 and table 4. The duration of the examination was 10 minutes with an equilibration of two minutes before the measurement (not included in the graph 10).

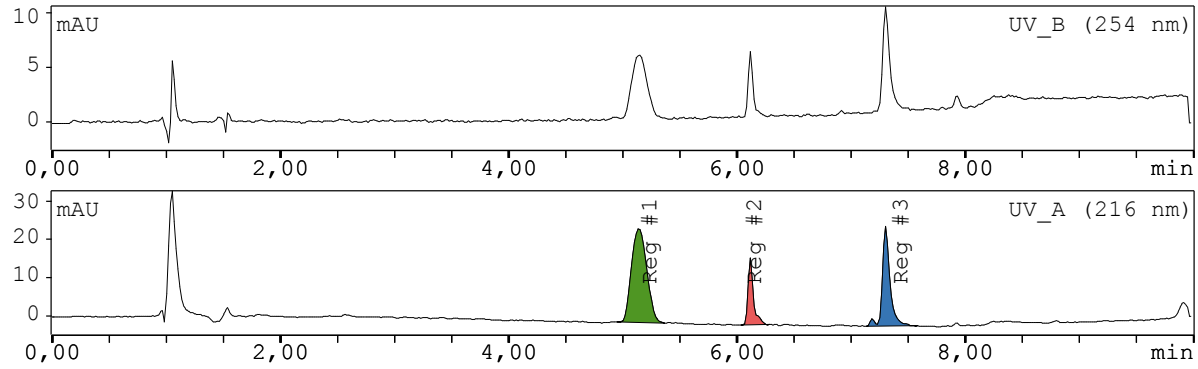

Figure 10: Representative HPLC chromatogram of telenzepine after 1 hour at 75°C with 6 M HCl and UV-detection at 254 nm (above) and 216 nm (below). The intermediate product appears at 5.13 min, the rearrangement product at 6.12 min and telenzepine at 7.31 min. Dead time was 1.07 min.

Elution time for telenzepine was at 7.31 min, its rearrangement product showed at 6.12 min and the dead time was 1.07 min. Starting with reaction conditions set to 55°C and HCl concentration of 0.5 M a third peak appeared after an hour reaction time which could be observed at 5.13 min and might be the intermediate product as described by Sturm *et al*.[36] The retention factor for telenzepine is 5.8, 4.7 for its rearrangement product and 3.8 for the intermediate product.

4.1.5 Calibration

After finding the respective HPLC gradient programs for the test substances calibration curves were generated. For all substances under investigation, solutions with the concentration of 100, 50, 10, 5, 1, 0.5, 0.1, 0.05 and 0.01 µg/mL were prepared and measured in three repetitions starting from the lowest concentration with injection volumes of 20 µL. For the calibration of pirenzepine the analytical reference standard of the European directorate for quality of medicines and healthcare (EDQM) was used and combined with its rearrangement product in one solution and measured simultaneously for a more efficient and simpler measurement. LOD and LOQ were calculated according to the guidelines of the International Council for Harmonisation of Technical Requirements for Pharmaceuticals for Human Use (ICH, topic Q 2 (R1)).[37]

4.1.6 Kinetic experiment

To estimate the reaction rate constant (k_i) for the rearrangement reaction of pirenzepine and its derivatives similar reaction conditions were chosen as described in section 4.1. 50 µL of the compound solutions were mixed with 50 µL of 0.2 M, 1 M and 12 M HCl for a final concentration of 0.1 M, 0.5 M and 6 M HCl in the reaction tubes. The reactions were conducted on a thermoshaker at temperatures of 37°C, 55°C and 75°C. Samples were taken after 0.5 h, 1 h, 1.5 h and 24 h. The sample sets from the 37°C measurements reacted for 66 hours due to the slow conversion. 5 µL of the reaction solution were carefully transferred into a glass inlay of the HPLC vial which contained 45 µL of the $NaHCO_3$ solution (55.55 mg/mL) and measured with the respective method. Afterwards, the conversion of the starting material to the rearrangement product was determined by the increase of area of the rearranged substances peak in the chromatograms over the monitored time. The resulting values were plotted as time VS. conversion graphs and a non-linear regression (one-phase association) of the plots yielded the reaction rate constants (k_i). For the calculation of the kinetic values pseudo-first order was

assumed. Afterwards, the logarithmized reaction rate constants and the inverted absolute temperatures were plotted and the resulting parameters of the linear function of the graphs represent the activation energy divided by the ideal gas constant (E_A/R) in the Arrhenius equation (eq. 14):[27]

$$\ln(k_i) = \ln(A) - \frac{E_A}{RT} \quad (14)$$

Equation 14: Logarithmized Arrhenius equation.

Kinetic experiments were conducted in triplicates and calculations for the reaction rate constant (k_i) were performed with *GraphPad Prism*.

4.1.7 Composition after quenching

The goal of this experimental setup was to investigate if the reaction solution continued the rearrangement reaction after quenching through the remaining carbonate and being stored at -20°C as all sample solutions were generally stored in a -20°C freezer until measurement if not used immediately. For this investigation three sample sets were created. The first one reacted with 0.2 M HCl and subsequentially quenched, the second one also reacted with 0.2 M HCl but left unquenched and the last set reacted with 12 M HCl and was quenched. After a reaction time of 50 minutes at 40°C the reaction solutions were immediately measured twice and then kept in the freezer at -20°C for two weeks to be measured again and compared.

4.1.8 Influence of different acids

These experiments aimed to determine if it was possible to achieve the same rearrangement of the compounds under investigation (sec. 4.1) in the presence of other acids than HCl and if all compounds were stable under those conditions. Therefore, sulphuric acid (H_2SO_4) and phosphoric acid (H_3PO_4) were used in a similar reaction which initiates the rearrangement of the compounds. 1 M and 6 M solutions of H_2SO_4 and 1 M and 8 M solutions of H_3PO_4 were prepared. 1:1 mixtures of compound solutions and acids in respective concentrations were prepared and reacted for 90 minutes at 50°C. Afterwards, the reaction solutions were examined with the respective HPLC methods.

4.1.9 logP measurement

The logP values of the compounds under investigation were examined with an adapted HPLC method from Donovan *et al*. described in Vraka *et al*.[38,39] For the measurement 250 µg of AFDX-384, 155 µg of telenzepine and 304 µg of the telenzepine rearrangement product were dissolved in 1 mL DMSO containing an internal standard (0.1 mg/mL triphenylene and 0.01 mg/mL toluene). 3 µL of the sample solutions were injected and measured on an apHERA column (fig. 11). Total run time of the logP method was 12 min with a three min equilibration phase before each measurement. The flow rate was set to 1.5 mL/min and a solvent gradient shown in table 5 at RT was used. The detector measured at 254 nm and 285 nm.

Table 5: Timetable and percentages of used solvents for the logP method.

Time [min]	0.01 M sodium phosphate buffer (pH 7.4) [%]	Methanol [%]
Initial	90	10
9.4	0	100
12	90	10

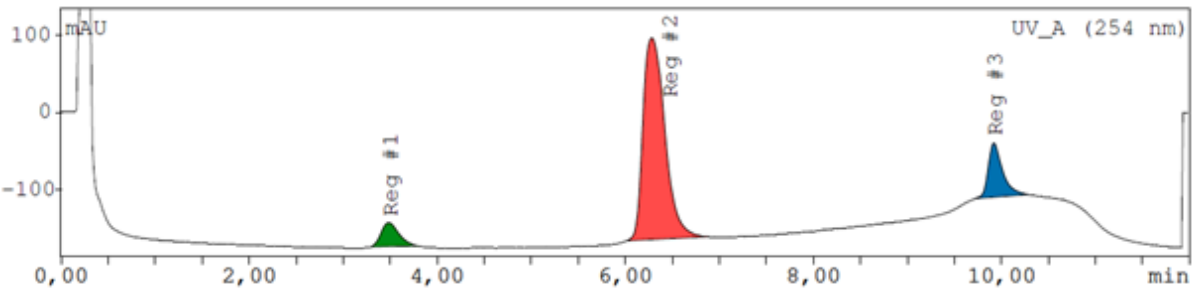

Figure 11: Representative HPLC chromatogram of the logP measurement of telenzepine with UV-detection at 254 nm. The green peak is telenzepine dihydrochloride, the red peak is toluene and the blue peak is triphenylene.

Finally, the logP value was calculated with formula 15 setting the measured retention time of the compound of interest in relation to the mean of the reference logP values of the two internal standards. As reference logP values for toluene and triphenylene the average literature values were taken from Donovan *et al.*:[38]

$$logP_{sub} = \frac{(logP_{tol} - logP_{tri}) * mRt_{sub} + mRt_{tol} * logP_{tri} - mRt_{tri} * logP_{tol}}{mRt_{tol} - mRt_{tri}} \quad (15)$$

Equation 15: Equation for the calculation of the HPLC logP value with $logP_{sub}$ being the resulting logP value of the substance of interest, mRt_{tol} and mRt_{tri} are the measured retention times of the internal standards toluene and triphenylene and $logP_{tol}$ and $logP_{tri}$ are the respective reference logP values.

4.1.10 Rearrangement under physiological conditions

For this HPLC experiment 5 mL of double concentrated simulated gastric fluid (SGF, tab. 6) for dissolution tests according to the European pharmacopeia (Phr. Eu., Ch. 4, Reagents) were prepared:[40]

Table 6: Composition of 5 mL double concentrated SGF according to the Phr. Eu.

5 mL double concentrated SGF	800 µL 1 M HCl 20 mg NaCl 32 mg of pepsin A 4200 µL purified H_20

Equal volumes of a 100 µg/mL of test substance solution and double-concentrated SGF were mixed and placed in a thermoshaker at 37°C. After starting the experiments, samples were taken 0.5 h, 1 h, 1.5 h, 6 h, 24 h, 30 h, 48 h, 54 h, 72 h and 78 h after the reaction had commenced. For comparison a similar setup was used simultaneously where a pirenzepine solution reacted with just 0.1 M HCl.

4.1.11 Analysis of pirenzepine samples derived from different producers

Nine different samples of pirenzepine were tested in an HPLC experiment to determine their chemical identity. Samples were ordered from the following suppliers:

- Abcam
- abcr GmbH
- AK Scientific
- Boehringer Ingelheim (Gastrozepin®)
- EDQM analytical reference standard

- Glentham Life Sciences
- Henan Allgreen Chemical Co. ltd./Wuhan BC. Oituo
- Sigma Aldrich
- TCI Chemicals

Solutions of all samples with the concentration of 1 mg/mL were prepared with purified water. Gastrozepin tablets were suspended in water to yield the same concentration and insoluble additives were removed by centrifugation and filtration prior to HPLC analysis. For the measurement 10 µL were injected onto the column of the HPLC and examined with the pirenzepine program from section 4.1.1.1.

4.2 Crystallization

In order to receive a crystalline product an adapted version of a vapour diffusion method described in Spingler *et al*. was chosen.[41] Solutions with the respective compounds were prepared and combined with the same volume of 12 M HCl. The mixtures were then placed in a thermoshaker at 75°C at 650 rpm, for their respective times (sec. 4.2.1 and 4.2.2). Afterwards, the reaction solutions were analysed with the corresponding HPLC separation programs to assure that the rearrangement product had formed. Then the solvent was removed under reduced pressure and the residues were taken up in a solvent according to Spingler *et al*. The reaction solution was subsequently transferred into a glass vial covered with a perforated lid and then placed into a 200 mL glass bottle which contained a corresponding antisolvent listed in Spingler *et al*. The top of the bottle was tightly screwed on and additionally sealed with parafilm. Finally, the setup was placed in a fridge and was checked for the first time after four days for crystal formation.

4.2.1 Telenzepine

For the crystallization of telenzepine 10.014 mg were dissolved in 750 µL purified water and then combined with 750 µL of 12 M HCl. After reaction of 18 h and evaporation as described in section 4.2 the residue, a white precipitation, was taken up in 1 mL methanol as the solvent and diethyl ether was chosen as the corresponding antisolvent. After four days in the fridge the crystallization setup was checked for the first time and long colourless needles had formed. Finally, 16 days after the initial reaction the crystals in their mother liquor were analysed.

4.2.2 AFDX-384

The first attempt to crystallize AFDX-384 was conducted by dissolving 5.197 mg of the compound in 750 µL ethanol. AFDX-384 reacted for 2 hours and was prepared as described in section 4.2. The residue, a yellow oil, was taken up in 1 mL of methanol as the solvent and diethyl ether was chosen as the antisolvent. Since after 11 days of the reaction no crystals had formed in the setup, samples of the crystallisation solution were taken for subsequent HPLC and MS measurements. Afterwards, the solvent of the crystallization solution was removed again under reduced pressure and for the second attempt the residue was dissolved in 0.5 mL methanol and placed in a n-hexane saturated environment. This setup was then also placed in the fridge. This combination also did not yield crystals after 11 days. Therefore, a third attempt was started from scratch where two reaction batches were started in parallel. In the first batch 3.648 mg AFDX-384 were dissolved in a 1:1 mixture of 250 µL EtOH (96%) and 250 µL 12 M HCl and the second batch consisted of 3.546 mg AFDX-384 in 0.5 mL of the same 1:1 EtOH (96%) and 12 M HCl mixture. Both batches reacted for 16 h at 75°C. As the antisolvent for batch one, a 1:1 combination of diethyl ether and acetone was chosen and dioxane for batch two. After 18 days the third and fourth attempt to obtain AFDX-384 crystals failed too.

Ultimately, the crystallization attempts for AFDX-384 were discontinued since no combination of solvent and antisolvent from the four attempts yielded a crystalline product.

4.3 Cell culture

Chinese hamster ovary (CHO) cells stable transfected with one of the five human muscarinic acetylcholine receptors subtypes ($M_1 – M_5$) were obtained from Missouri University of Science and Technology cDNA Resource Center (Cell Catalog#: CEM1000000, CEM2000000, CEM3000000, CEM4000000, CEM5000000)) and all required chemicals and solutions were purchased from *Gibco® Life Technologies*.

4.3.1 Cell line cultivation

Following conditions were used for CHO cells (tab. 7):

Table 7: Composition of the cell medium and selected conditions of the incubator for the storage of the CHO cells.

Temperature	37°C
Atmosphere	Humidified 5% CO_2
Medium	Ham's F-12(1X) Nutrient Mix Medium 10% foetal bovine serum 1% L-glutamine 2.75 mL geneticin (G418)
Storage	Cell culture flasks

To ensure proper growth of the cells the content must be split periodically after reaching approximately 90% confluency. Therefore, the cell culture flasks were checked under a microscope and then placed in a laminar flow cabinet. After removing the old medium, the flask was washed with PBS. Then 0.05% trypsin solution was added and placed for 5 minutes into the incubator to detach the cells from the bottom of the flask. Medium was added to incapacitate the enzyme and by pipetting a cell suspension was received. For cell line splitting 1 mL of the cell suspension was kept and the rest was discarded. Finally, fresh medium was added to the flasks, shaken and then placed back in the incubator.

4.3.2 Preparation of membrane suspension

To prepare a batch for the harvest of cells for the membrane suspension ten cell culture flasks were filled with fresh medium and to each 1 mL of CHO cell suspension was added and cultivated until 90% confluency was obtained. For the processing of the membrane suspension an adapted version of the procedure from Klotz *et al*. was used.[42] Before the procedure the ultracentrifuge was cooled to 4°C. The following steps were performed on ice or cooling packs. Buffer 1 and 2 (tab. 8), a PBS solution as well as a 1:50 protease inhibitor cocktail P2714 solution from *Sigma Aldrich* (content of a vial dissolved in 10 mL purified water for a 10-fold concentrated solution, aliquoted as 200 µL units, stored at -20°C) were placed on ice.[33,34]

Table 8: Composition of the two buffer solutions used in the preparation of the membrane suspension.

Buffer 1	10 mM Tris 1 mM EDTA pH 7.4 adjusted with HCl
Buffer 2	50 mM Tris pH 7.4 adjusted with HCl

A culture flask was taken out of the incubator and placed on top of a cooling pack. Firstly, the old medium was discarded and then the flask was washed with PBS. Next, 2 mL of buffer 1 were added and the CHO cells were scraped off. The cell suspension was transferred to a 5 mL Eppendorf tube on ice already filled with 400 µL of protease inhibitor cocktail P2714 solution. The content of a second flask was added after it was processed just as describe above. These steps were repeated for the ten flasks of a batch. After transferring the cell suspensions into the tubes, they were homogenized with an insulin syringe and then centrifuged for 10 minutes at 4°C at 1000 g. The resulting supernatant was transferred to a SETON-tube and ultra-centrifuged for 40 minutes at 4°C at 100 000 g. This time the supernatant was discarded, and each pellet was suspended in 250 µL of ice-cold buffer 2. The yielded membrane solutions were merged in one cryovial and stored at -80°C.

4.4 Harvester experiments

For the competitive displacement experiments [N-methyl-^{3}H]-scopolamine methyl chloride ([^{3}H]NMS, Perkin Elmer, 37 MBq, 2.964 TBq/mmol in 1 mL ethanol) was chosen as the radioligand (RL) because of its high affinity towards all receptor subtypes and its availability as a tritiated molecule. Still due to different affinities towards the receptor subtypes, [^{3}H]NMS was prepared in aliquots in different concentrations of the RL as described in table 9.

Table 9: Respective concentrations of the [^{3}H]NMS radioligand aliquots for the competitive displacement experiments for each mAChR subtype.

mAChR subtype	M_1	M_2	M_3	M_4	M_5
Concentration of RL	2 nM	3 nM	8 nM	2 nM	10 nM

Further, stock solutions of the test substances were prepared by a serial dilution to obtain the concentrations of 5 mM, 1 mM, 500 µM, 100 µM, 50 µM, 10 µM, 5 µM, 1 µM, 500 nM, 100 nM, 50 nM, and 10 nM in purified water. The solutions with the compounds of interest were concentrated 100-fold so that the final concentration in the tubes would be between 50 µM and 0.1 nM. Firstly, the compounds were screened using the concentrations of 10 µM, 1 µM, 100 nM, 50 nM, and 10 nM to determine the concentration range which yielded a consistent sigmoid curve in proximity to the inflection point. Subsequently, the found concentration ranges were applied in the displacement experiments for the respective compounds. An aliquot of the corresponding [^{3}H]NMS radioligand and membrane solution were thawed. Then the membrane solution was resuspended in membrane buffer, so that the final volume would add up to 17 mL (concentration of the membrane varied from batch to batch and were dependant on the chosen receptor subtype).

Table 10: Composition of the membrane and washing buffer for the Harvester experiments.

Membrane buffer	50 mM Tris pH 7.4 adjusted with HCl
Washing buffer	50 mM Tris 1 mM EDTA 10 mM $MgCl_2$ pH 7.4 adjusted with HCl

A Brandel 36-rack filled with tubes was prepared. In each tube 5 µL of the test substance solution, 50 µL of radioligand, and 445 µL of the membrane solution were added and

equilibrated for 90 minutes. In the meantime, a Brandel filter (GF/B) was blocked with 1% polyethyleneimine (PEI) solution and the device was pre-washed with washing buffer (tab. 10). After 90 minutes the filter was inserted into the harvester and the content of each tube was sucked onto its position on the filter and washed twice with one third of the volume of a tube. Next, the areas of the filter with the membrane solution on it were punched out with the intended appliance into the tubes for the beta counter. 2 mL of Ultima Gold™ scintillation cocktail was added to the tubes and incubated for 30 minutes on a shaker with a low setting. The tubes were placed in the beta counter and measured for a minute each. All concentrations were measured in triplicates with three replicates each. Afterwards, IC_{50}-values were calculated with the mathematics program *GraphPad Prism 6 via* the "one site – Fit logIC50". Finally, the IC_{50} values were taken to calculate the binding affinity of the compounds (K_i) towards the respective mAChR subtypes using the Cheng-Prusoff equation (eq. 13).[31]

5 Results and discussion

5.1 HPLC experiments

5.1.1 Calibration

5.1.1.1 Pirenzepine

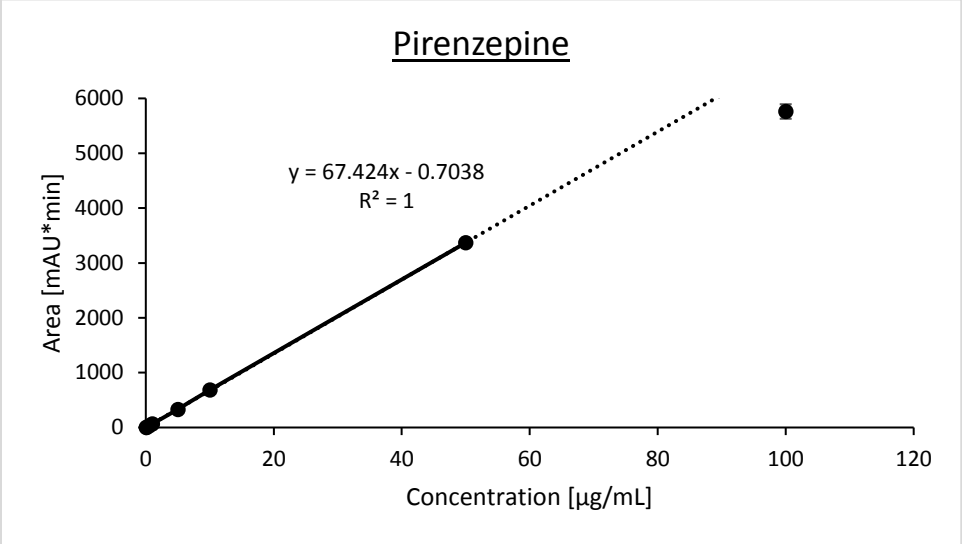

Figure 12: Calibration curve for pirenzepine. The standard deviation is displayed by the error bars but only the standard deviation range of the 100 µg/mL data point is large enough to be displayed.

The calibration curve for pirenzepine (fig. 12) yielded a LOD of 0.30 µg/mL and a LOQ of 0.90 µg/mL for the range from 0.05 µg/mL to 50 µg/mL. This calibration curve was utilized for the respective concentration calculations. In figure 12 only the standard deviation error bars for the 100 µg/mL data point are large enough to be visible.

5.1.1.2 Pirenzepine rearrangement product

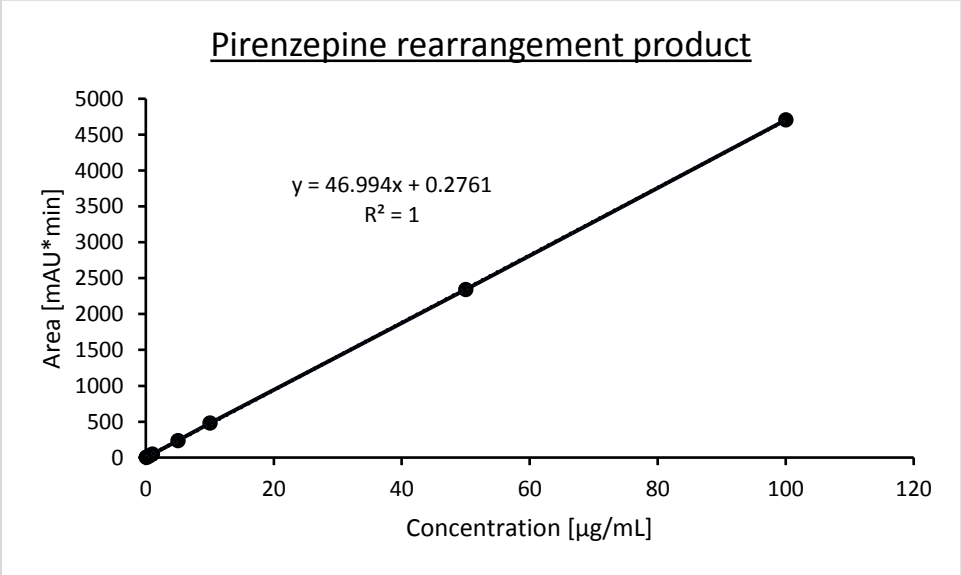

Figure 13: Calibration curve for the pirenzepine rearrangement product. The standard deviation error bars are too small to be displayed.

Figure 13 shows that the linear range for this function applied from 0.05 µg/mL to 100 µg/mL with a LOD of 0.41 µg/mL and LOQ of 1.23 µg/mL. To determine if the rearrangement is quantitative the initial concentration of pirenzepine was compared to the final concentration of

the pirenzepine rearrangement product from the pirenzepine kinetics experiments (sec. 5.1.2). The standard deviation error bars for all data points were too small to be displayed in figure 13. The results showed that for the reaction conditions of 55°C with 6 M HCl after 24 h 95% were converted to the rearrangement product. The 75°C sample set with 6 M HCl showed after 24 h that pirenzepine was completely converted to its rearrangement product.

5.1.1.3 AFDX-384

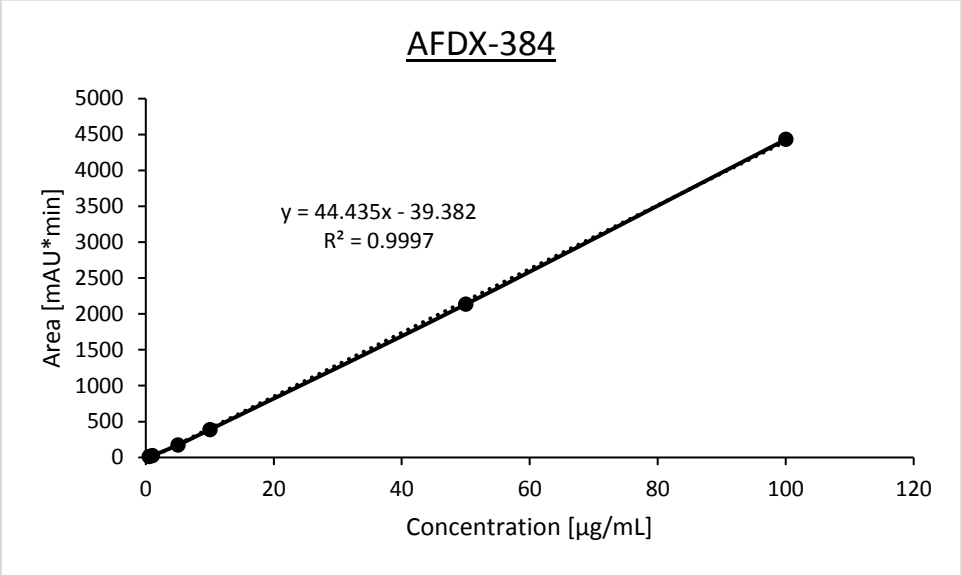

Figure 14: Calibration curve for AFDX-384. The standard deviation error bars are too small to be displayed.

Linearity for the AFDX-384 calibration curve was valid from 0.5 to 100 µg/mL with a LOD of 3.19 µg/mL and LOQ of 9.68 µg/mL. Again, the standard deviation error bars in figure 14 for all data points were too small to be displayed. This function was used for further determinations of concentrations in the following chapters for AFDX-384.

5.1.1.4 Telenzepine

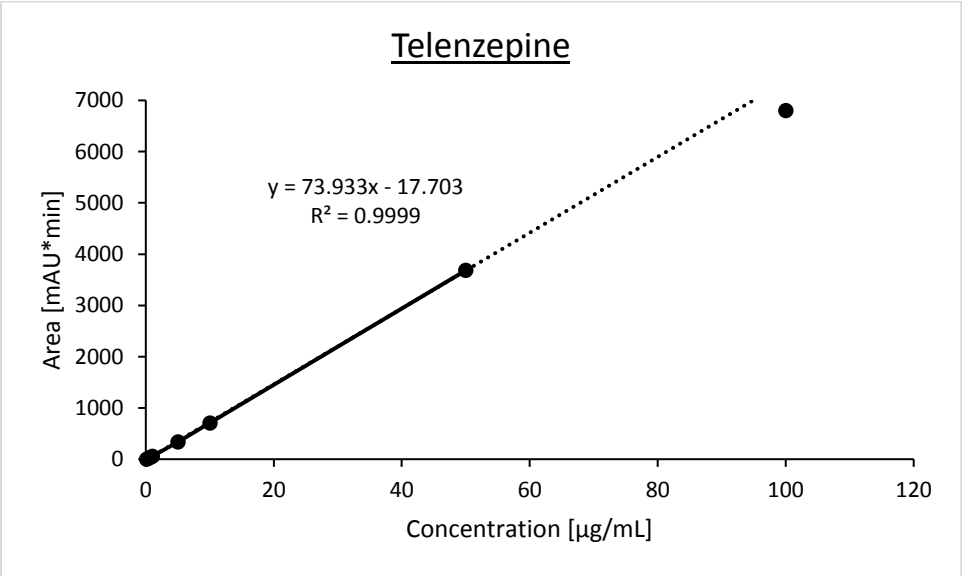

Figure 15: Calibration curve for telenzepine. The standard deviation error bars are too small to be displayed.

The resulting calibration curve for telenzepine yielded a function with linearity from 0.1 to 50 µg/mL and LOD of 0.74 µg/mL and LOQ of 2.24 µg/mL. All standard deviation error bars in

figure 15 are too small to be visible. In the following sections this calibration was used to calculate the concentrations of telenzepine in the experiments.

5.1.2 Kinetic experiments

Chemical kinetics experiments were conducted to gain information on the reaction mechanisms of the acidic rearrangement of the compounds under investigation. A model reaction mechanism was constructed with the rearrangement reaction following pseudo-first order kinetics due to the protons of present HCl being in excess and thus at steady state.

5.1.2.1 Pirenzepine

For the calculations of the kinetic parameters the sample sets which reacted with 6 M HCl were chosen as they exhibited more pronounced curves.

Table 11: Mean conversion values in percent for their respective temperature and reaction time.

Mean conversion [%]	After 30 min	After 60 min	After 90 min
37°C	2.2 ± 0.2	4.9 ± 0.2	7.3 ± 0.1
55°C	14.8 ± 1.4	29.6 ± 2.6	43.1 ± 3.6
75°C	58.1 ± 2.6	81.3 ± 1.7	91.2 ± 3.8

With these values the kinetic profiles of the pirenzepine rearrangement at different temperatures (tab. 11 and fig. 16) were created and through a nonlinear regression the reaction rate constants k_i were obtained (tab. 12).

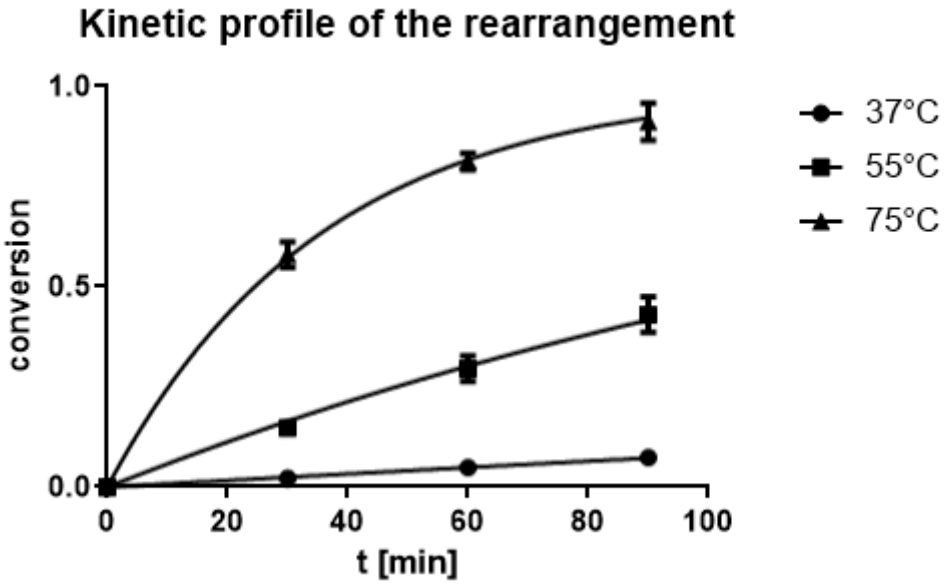

Figure 16: Mean kinetic profiles of the pirenzepine rearrangement reaction according to their respective temperature settings. Error bars represent standard deviation, with some error bars being too small to be displayed properly.

Table 12: Mean reaction rate constants from the 6 M HCl sample set for each respective temperature.

Temperature [°C]	k_i [mol/L s]
37	$8.4 * 10^{-4} \pm 0.2 * 10^{-4}$
55	$6.0 * 10^{-3} \pm 0.6 * 10^{-3}$
75	$2.8 * 10^{-2} \pm 0.2 * 10^{-2}$

The logarithmized mean reaction rate constants were plotted against the inverted absolute temperature which created the linear Arrhenius plot from which the activation energy was calculated.

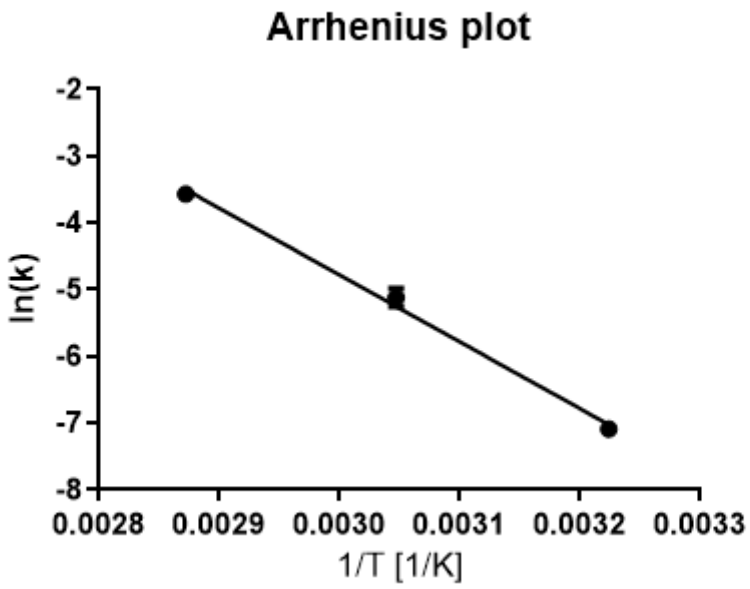

Figure 17: Resulting mean Arrhenius plot of the 6 M HCl sample sets.

The resulting graph (fig. 17) yielded a mean activation energy (E_A) for the rearrangement reaction of pirenzepine of 83.2 ± 1.9 kJ/mol.

5.1.2.2 AFDX-384

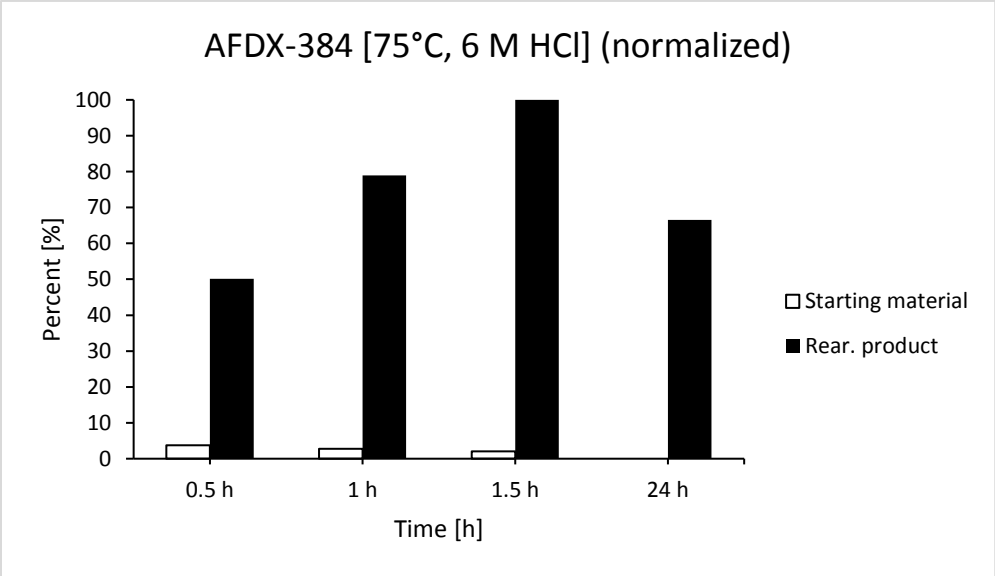

Figure 18: Normalized bar graph of the AFDX-384 kinetic sample reacting with 6 M HCl at 75°C.

Figure 18 showed that at reaction conditions of 24 h with 6 M HCl and 75°C led to loss of the rearrangement product, but with 90 minutes AFDX-384 was already almost completely converted to its rearrangement product. Therefore, reaction time for the rearrangement of

AFDX-385 for the crystallization attempt (sec. 4.2.2) was set to two hours. Further, due to the decomposition of the rearrangement product during the experiment pseudo first order did not apply and the measurement of the kinetic parameters of AFDX-384 was discontinued.

5.1.2.3 Telenzepine

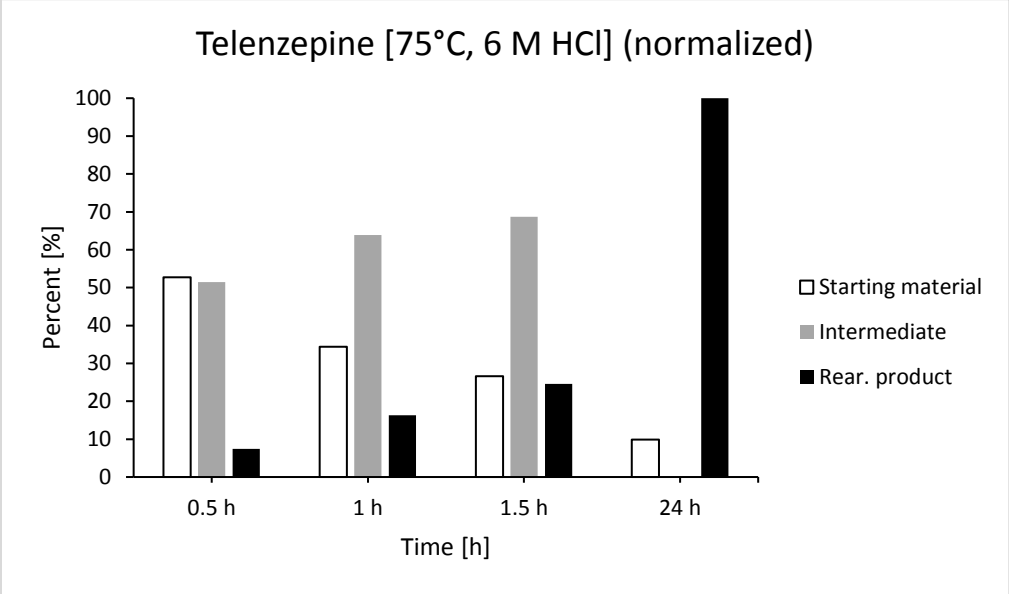

Figure 19: Normalized bar graph of the telenzepine kinetic sample reacting with 6 M HCl at 75°C.

Figure 19 displayed that after 24 hours the starting material was almost completely converted to the rearrangement product of telenzepine. As mentioned in section 4.1.4 with reaction conditions of 55°C and 0.5 M HCl a detectable intermediate product was measured which also showed that pseudo first order kinetics did not apply and therefore the measurement of the kinetic parameters of telenzepine were discontinued as well.

5.1.3 Composition after quenching

The purpose of these experiments was to examine if the composition of the samples from the rearrangement reaction changed when stored as quenched solutions in a -20°C freezer and if the remaining carbonate reacts with the starting material or its rearrangement product. Hence, after two weeks in a -20°C freezer the reaction solutions were measured again for changes in the composition of their contents and compared to the results of the measurements directly after the reaction.

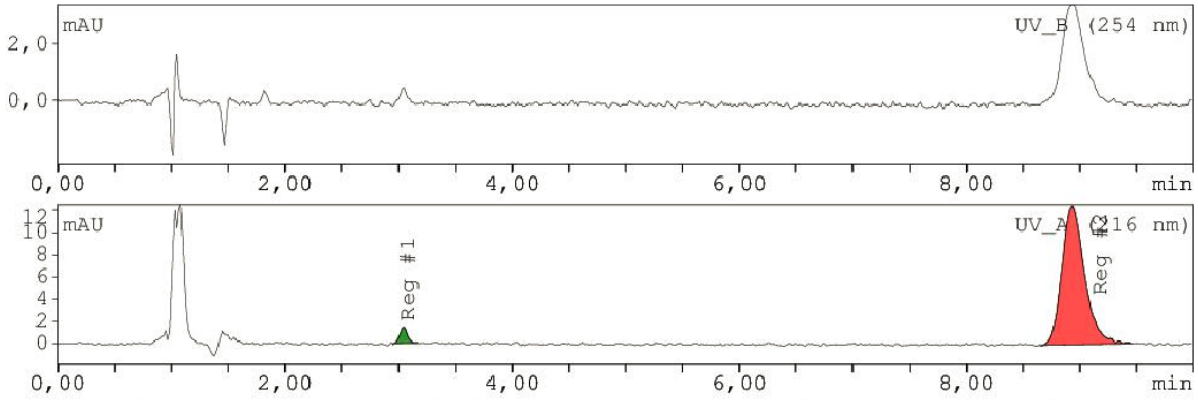

Figure 20: Quenched pirenzepine sample measured directly after 50 minutes reaction time with 6 M HCl at 40°C.

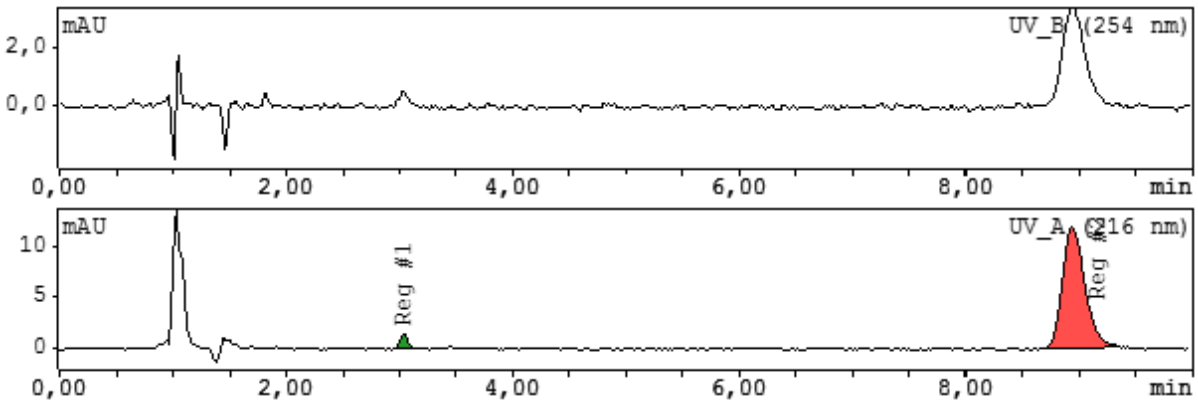

Figure 21: Quenched pirenzepine sample (50 min, 6 M HCl, 40°C) measured after two weeks of storage.

Table 13: Comparison of the area values of the quenched 6 M HCl samples directly measured after reaction and after two weeks storage time. PR: pirenzepine rearrangement product, pir.: pirenzepine starting material.

Pirenzepine sample	Area PR. [min*mAU]	Area pir. [min*mAU]
6 M HCl, quenched, directly after reaction (1)	7.4	167.8
6 M HCl, quenched, directly after reaction (2)	6.6	172.7
6 M HCl, quenched, directly after reaction (mean)	7.0 ± 0.4	170.3 ± 2.5
6 M HCl, quenched, two weeks storage (1)	8.0	170.4
6 M HCl, quenched, two weeks storage (2)	6.2	166.4
6 M HCl, quenched, two weeks storage (mean)	7.1 ± 0.9	168.4 ± 2.0

Table 13 and comparing the chromatograms from figures 20 and 21 showed a difference of 1.1% in measured area for the pirenzepine peak and 1.4% for the pirenzepine rearrangement product. Therefore, changes in the composition after quenching and storing at -20°C can be considered negligible and the rearrangement reaction does not continue under those conditions.

5.1.4 Influence of different acids

The rearrangement reaction under similar conditions as in section 4.1. was examined, however in this case acids other than HCl, namely phosphoric and sulfuric acid, were used. The goal was to determine if the rearrangement was possible using different acids and to obtain information about the stability of pirenzepine, AFDX-384 and telenzepine regarding these acids. The reaction was conducted for 90 minutes at 50°C with 1 M and 8 M H_3PO_4 was well as 1 M and 6 M H_2SO_4. The results of these experiments showed that the same rearrangement for all compounds of interest could be achieved under these conditions. For a better presentation each group of substances was normalized individually:

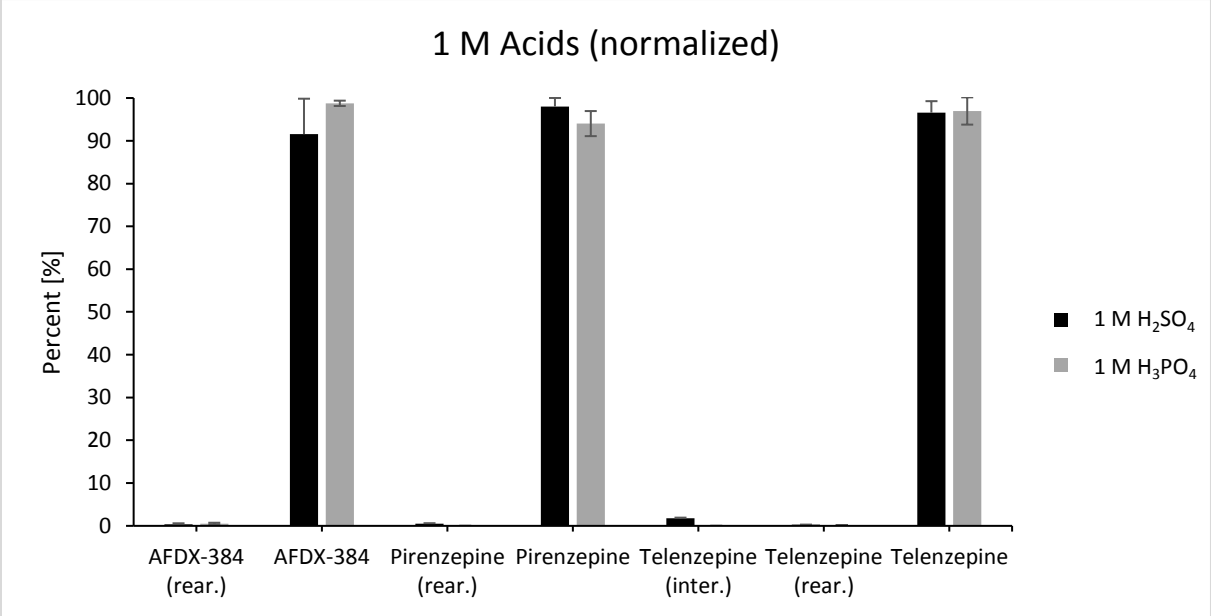

Figure 22: Normalized bar graph of pirenzepine, AFDX-384, telenzepine and their rearrangement products after reacting with 1 M phosphoric and sulfuric acid respectively. Error bars represent standard deviation with some error bars being too small to be displayed.

The graphs of figure 22 display a side by side comparison of the results for each substance and their rearrangement products which reacted with 1 M of H_3PO_4 and H_2SO_4. At this acid concentration the conversion of the starting materials to their rearrangement products is comparable. Although, for the reaction with 1 M of H_2SO_4 more of the rearrangement product was observed. In contrast, after the reaction time of 90 minutes with 1 M H_3PO_4 neither the rearrangement product of pirenzepine nor the intermediate product of telenzepine were detected.

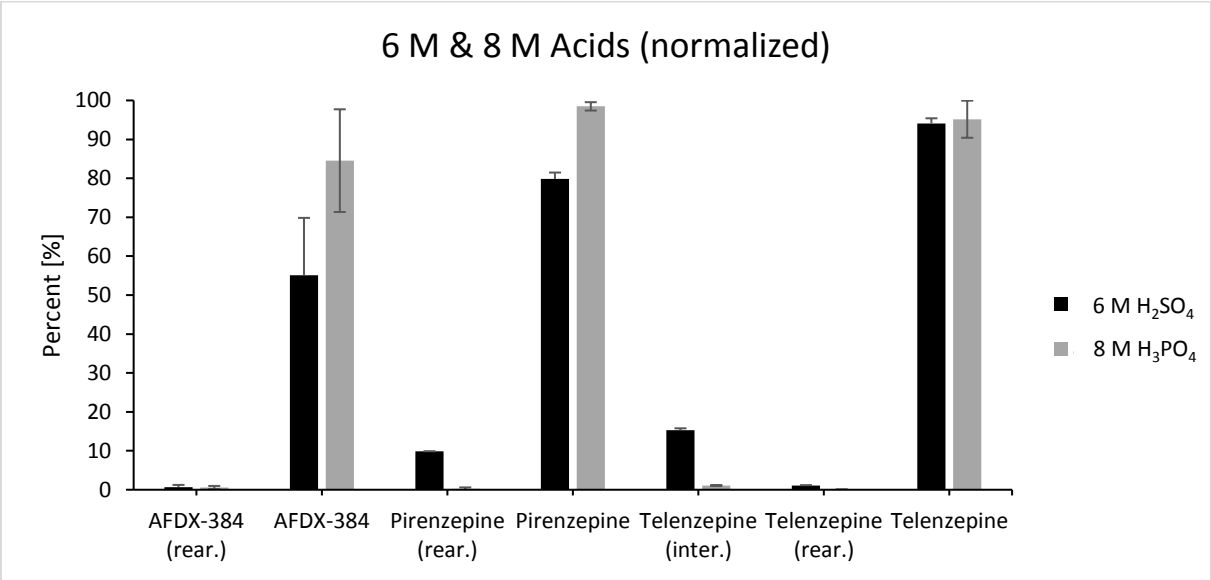

Figure 23: Normalized bar graph of pirenzepine, AFDX-384, telenzepine and their rearrangement products after reacting with 8 M phosphoric and 6 M sulfuric acid respectively. Error bars represent standard deviation with some error bars being too small to be displayed.

The results for the concentration of 6 M H_2SO_4 and 8 M H_3PO_4 (fig. 23) supported the observed trend from the reactions with the 1 M acids. Again, after 90 minutes reaction time with 6 M H_2SO_4 less starting material and more rearrangement product could be measured compared to the reaction with 8 M H_3PO_4. The observation, that the rearrangement happened faster with H_2SO_4 and slower with H_3PO_4 might indicate an influence of the strength of the acid on the rearrangement process.

5.1.5 logP measurement

Table 14: Obtained logP values for all substances of interest and their rearrangement products.

Compound	HPLC method	Data base values
Pirenzepine	-0.70 ± 0.54	0.6 [43]
Pirenzepine (rear.)	-1.48 ± 0.65	N/A
AFDX-384	1.76 ± 0.20	3.84 [44]
Telenzepine	0.40 ± 0.38	0.37 [45]
Telenzepine (rear.)	0.18 ± 0.42	N/A

The logP value is a physicochemical parameter which describes the lipophilic properties of compounds influencing their inherent adsorption, distribution, metabolism, excretion and toxicity.[46] One possibility to interpret this contrast in measured and database logP values (tab. 14) lies within the chosen method itself. According to the OECD's guideline for the testing of chemicals (Test no. 117) the logP HPLC experiments cover a range of 6 to 0 for logP values and therefore the examined compounds might be too hydrophilic putting them outside of the range for this method, which uses the substances toluene (logP = 2.74) and triphenylene (logP = 5.49) as references.[47] Another reason for the inherent difference in comparing the measured logP values to the ones from databases might derive from the issue that the database values are calculated for the water/octanol method. However, a general trend for the rearrangement products of pirenzepine and telenzepine was observed. Both logP values shifted to more hydrophilic properties after the rearrangement of the starting material. As a result, the *in vivo* absorption and distribution will have decreased, and the substances would be even less likely to penetrate the BBB.[46] Conversely, to make assumptions about the metabolization and clearance as well as toxicity of the rearrangement products additional data and parameters must be taken into account.[46]

5.1.6 Rearrangement under physiological conditions

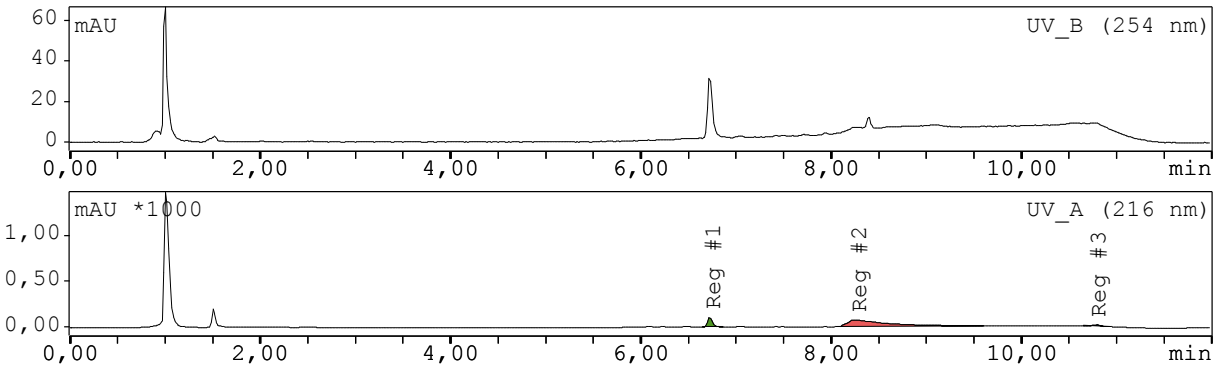

Figure 24: Representative chromatogram of pirenzepine after 30 minutes reaction time under physiological conditions with SGF.

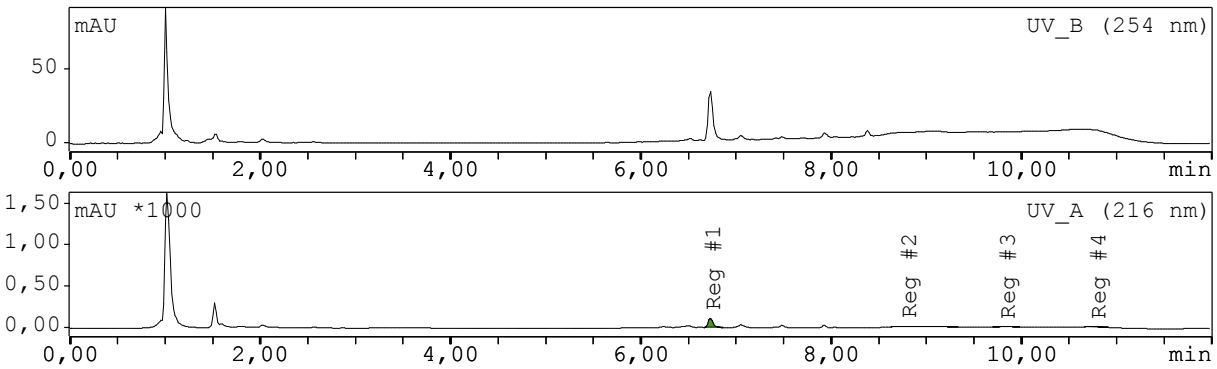

Figure 25: Representative chromatogram of pirenzepine after 72 hours reaction time under physiological conditions with SGF.

Table 15: Table of the mean areas of the substances after reacting for 0.5 and 72 hours with SGF under physiological conditions.

Compound	Mean area [min*mAU]
Pirenzepine (SGF) 0.5 h	338.5 ± 3.3
Pirenzepine (SGF) 72 h	381.7 ± 16.5
Pirenzepine (HCl) 0.5 h	158.3 ± 13.9
Pirenzepine (HCl) 72 h	156.5 ± 10.4
AFDX-384 (SGF) 0.5 h	199.3 ± 2.9
AFDX-384 (SGF) 72 h	232.4 ± 27.7
Telenzepine (SGF) 0.5 h	392.1 ± 0.8
Telenzepine (SGF) 72 h	421.7 ± 6.3

One aspect of this experimental setup which should be answered was if pepsin might have an influence on the rearrangement of the compounds. A concentration of 100 µg/mL of either pirenzepine or AFDX-384 or telenzepine was chosen generally for the test solutions so that the final concentration after mixing it with acid 1:1 would be at 50 µg/mL which would be equal to the recommended intake of Gastrozepin® on an empty stomach according to the package leaflet.[9,10,48] Comparison of all sample sets (tab. 15) showed that after 72 hours of reaction time no rearrangement products could be detected. In light of these findings and considering the results from the kinetic experiments (sec. 5.1.2.1) administration of pirenzepine poses no imminent danger of rearrangement in the stomach for humans. Contrasting the chromatograms (fig 24 and 25, 216 nm) clearly shows a gradual recession of the peak band after minute 8 over the course of the measurements. This indicated that pepsin underwent autolysis under the chosen conditions rather than influencing the rearrangement.[49] Furthermore, the rearrangement of pirenzepine under physiological conditions is even more unlikely considering the passing times of orally administered drugs depending on their dissolution and hydrophobic properties. The longest dwelling time of a substance in the stomach is up to few hours and is therefore not enough time for the rearrangement of the compounds to occur under the chosen conditions of this experiment.[50]

5.1.7 Proposed acidic rearrangement of pirenzepine

When evaluating commercially obtained pirenzepine regarding its potential as a M_1 selective PET tracer for the peripheral nervous system, a literature unknown by-product was discovered (unpublished data). The following investigation revealed that the compound might have been synthesized with similar conditions as described in the patent CN103044419A (120°C, 3 MPa,

conc. HCl, autoclave). With these findings the theory of an acidic rearrangement was proposed (fig. 26):

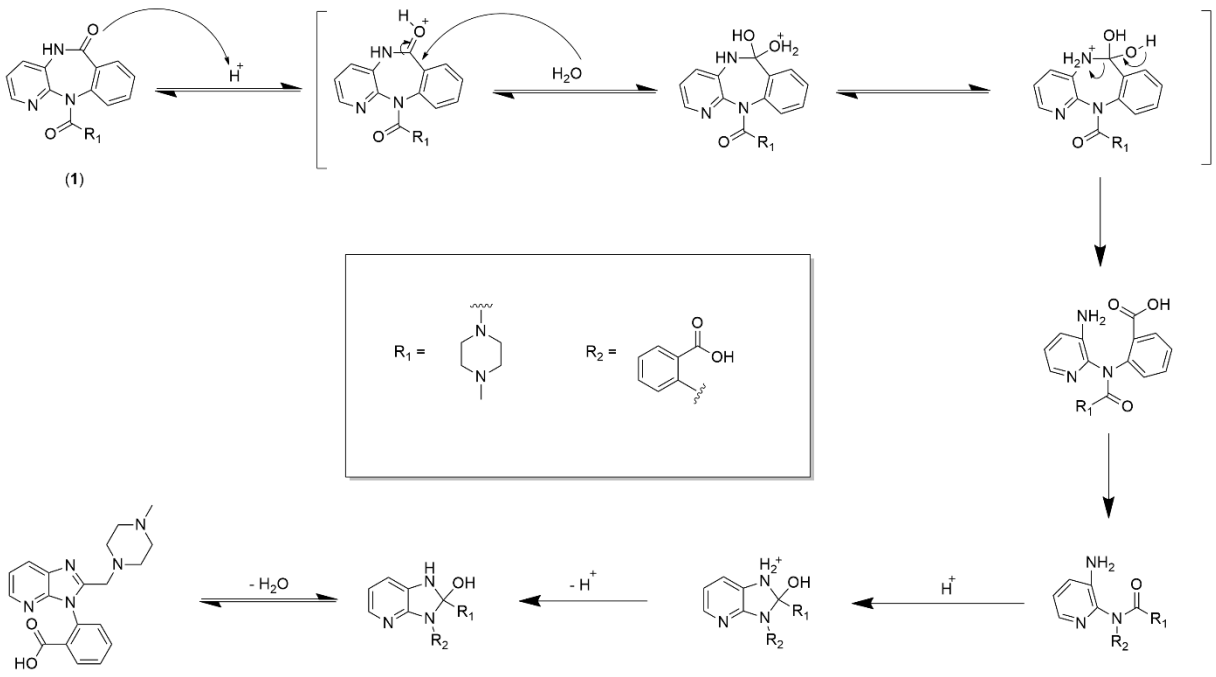

Figure 26: Proposed mechanism for the rearrangement of pirenzepine in an acidic environment.

The starting point for the suggested rearrangement would be an acid catalysed cleavage of the amide function which is then followed by an imine formation. Due to the structural homology of AFDX-384 (sec. 1.2.2) and telenzepine (sec. 1.2.3) to pirenzepine the compounds were expected to perform a similar rearrangement reaction in an acidic environment.

5.1.8 Analysis of pirenzepine samples derived from different producers

Table 16: Results of the qualitative examination of the pirenzepine samples from different distributors.

Company	Correct product
Abcam	Yes
abcr GmbH	No
AK Scientific	No
Boehringer Ingelheim (Gastrozepin®)	Yes
EDQM reference standard	Yes
Glentham Life Sciences	Yes
Henan Allgreen Chemical Co. ltd./ Wuhan BC. Oituo	Yes
Sigma Aldrich	Yes
TCI Chemicals	Yes

Nine commercially available pirenzepine samples were tested for the presence of the rearrangement product in the chemicals. All samples except for the drug Gastrozepin® where intended for research only by the respective distributors. Therefore, HPLC measurements were conducted in a qualitative way (tab. 16). All tested samples showed that the correct product was delivered except for those from *abcr GmbH* and *AK Scientific*. The HPLC method used for

pirenzepine identified those two samples as pirenzepine's rearrangement product. Hence, the distributors were informed, and the wrongly labelled substance was suspended form their product catalogue.

5.2 Crystallization

5.2.1 AFDX-384

Table 17: All combinations of solvent and antisolvent from each crystallization attempt of AFDX-384.

Attempt	Solvent	Antisolvent
1	Methanol	Diethyl ether
2	Methanol	n-Hexane
3	1:1 12M HCl and 96% EtOH	1:1 Diethyl ether and acetone
4	1:1 12M HCl and 96% EtOH	Dioxane

With all combinations of solvent and antisolvent from table 17 only yellow oil could be obtained. For each crystallisation attempt after 11 days no crystals had formed therefore samples of the crystallisation solution were taken for HPLC and MS analysis. The resulting chromatogram of the solution of the first AFDX-384 crystallisation attempt is presented in figure 27:

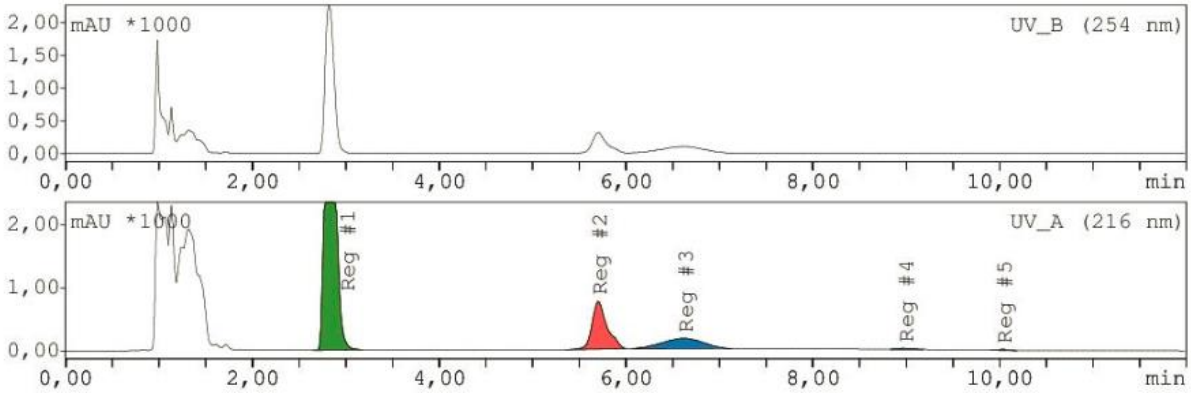

Figure 27: Chromatogram of AFDX-384 after 11 days for the first crystallization attempt.

The chromatogram showed that only 0.24% of the initial amount of AFDX-384 rearrangement product could be detected. The measured MS from the same sample of the crystallization solution is depicted in figure 28:

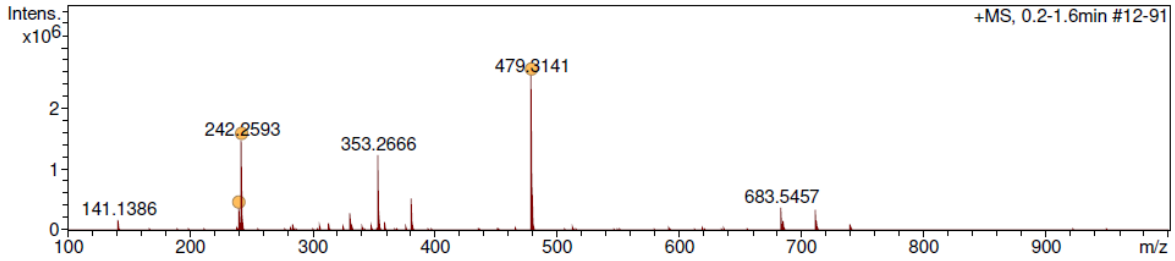

Meas. m/z	#	Ion Formula	m/z	err [ppm]	mSigma	# mSigma	Score	rdb	e⁻ Conf	N-Rule
141.1386	1	C8H17N2	141.1386	0.5	7.2	1	100.00	1.5	even	ok
240.1601	1	C13H22NO3	240.1594	-2.9	58.4	1	100.00	3.5	even	ok
242.2593	1	C14H32N3	242.2591	-1.1	15.3	1	100.00	0.5	even	ok
479.3141	1	C27H39N6O2	479.3129	-2.5	26.5	1	100.00	11.5	even	ok
	2	C31H43O4	479.3156	3.1	35.5	2	89.19	10.5	even	ok
	1	C29H44NaO4	479.3132	-1.9	24.2	1	100.00	7.5	even	ok
	2	C30H40N4Na	479.3145	0.9	40.7	2	64.23	12.5	even	ok

Figure 28: Mass spectrum of the reaction solution of the first crystallization attempt.

The base peak of 479.3141 m/z represents AFDX-384. 353.2666 m/z and 683.5457 m/z were contaminations of the MS system which could not be removed. Checking the 242.2593 m/z peak with a mass calculator suggested that this mass could result from fragmentation at the carbamate moiety. The results of the HPLC and MS measurements showed that the AFDX-384 rearrangement product was not stable under the chosen conditions for the crystallisation and all other crystallisation attempts yielded similar results. After four different crystallization attempts for the rearrangement product of AFDX-384 it was not possible to obtain a crystalline product and therefore the rearranged AFDX-384 could not be isolated. Subsequently, further characterization and the displacement experiments could not be conducted.

5.2.2 Telenzepine

The combination of methanol and diethyl ether delivered crystals for the telenzepine rearrangement product in the shape of long colourless needles after four days in a fridge. After a total of 16 days of crystallization the rearranged telenzepine was measured *via* XRD:

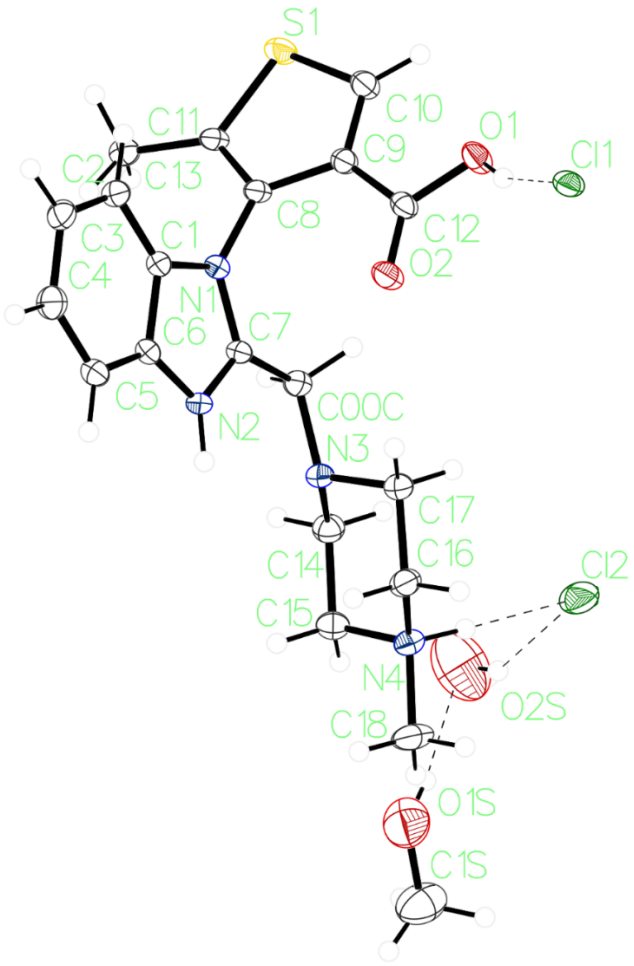

Figure 29: Crystal structure of the dihydrochloride telenzepine rearrangement product.

Figure 29 shows that the rearranged telenzepine crystallized as dihydrochloride.

5.3 Other measurements

IR measurements were conducted for pirenzepine and its rearrangement product with the goal to find a quick and reliable method which could be implemented in quality assurance. Furthermore, NMR spectra were recorded for additional characterization of a literature unknown compound.

5.3.1 IR measurements of pirenzepine

As a mean to quickly distinguish between the starting material and its rearrangement product an IR-ATR measurement was conducted. Hence, pirenzepines and its respective rearrangement products fingerprint region ranging from 1750 - 600 cm^{-1} were measured with a resolution of 2 cm^{-1}.

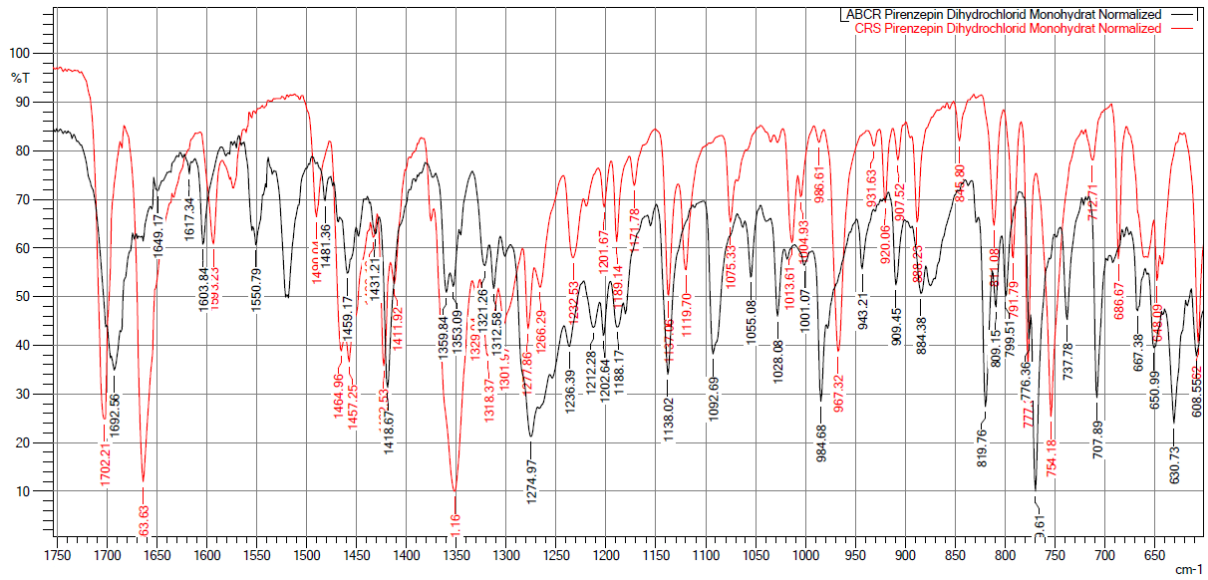

Figure 30: Normalized IR-ATR spectra of pirenzepine (red) and its rearrangement product (black) displayed in the fingerprint region from 1700 - 600 cm^{-1} with a resolution of 2 cm^{-1}.

Figure 30 shows that the chosen settings for the IR-ATR measurement provide a distinguishable spectrogram of the pirenzepine and its rearrangement product. The most prominent peaks of the IR-ATR spectra of pirenzepine and its rearrangement product are listed in table 18:

Table 18: Distinct peaks in the fingerprint range from 1700 – 600 cm^{-1} of pirenzepine and its rearrangement product found in the IR-ATR spectra.

	Peak (cm^{-1})
Pirenzepine	1702.21
	1663.51
	1464.96
	1457.25
	1351.16
	967.32
	754.18
Pirenzepine (rear.)	1692.56
	1550.79
	1274.97
	1092.69
	984.68
	819.76
	763.61
	707.89
	630.73

5.3.2 NMR measurement of the telenzepine rearrangement product

After obtaining the crystal structure of the telenzepine rearrangement product, the substance was further characterized through ^{1}H- and ^{13}C-NMR (fig. 31 and 32).

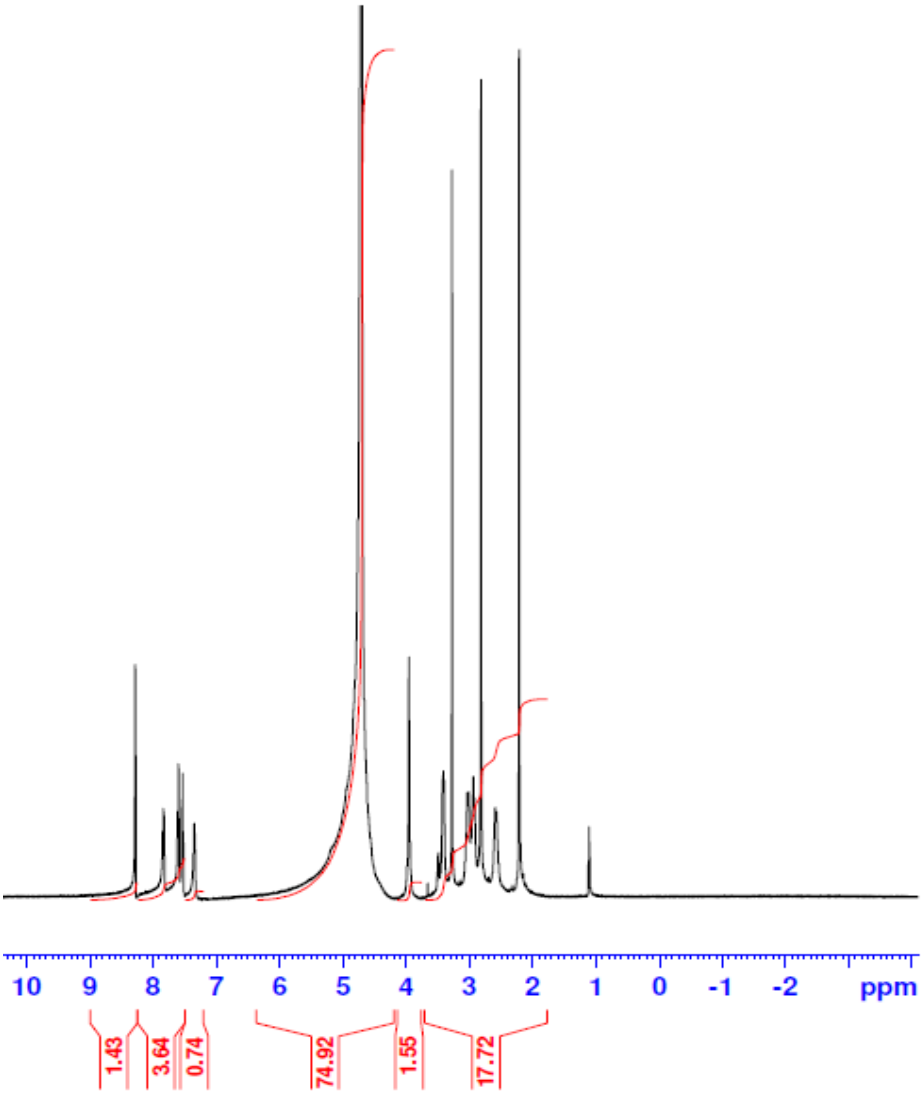

Figure 31: [1]H-NMR of the telenzepine rearrangement product measured with a resolution of 600 MHz in D_20.

[1]H-NMR (600 MHz, D_2O) δ 8.37 (d, 1H, *J*=2.3 Hz, thiophene H-2), 7.92 (d, 1H, *J*=7.1 Hz, Ar H-4), 7.68 (t, 1H, *J*=7.1 Hz, Ar H-5), 7.62 (t, 1H, *J*=7.1 Hz, Ar H-6), 7.43 (d, 1H, *J*=7.1 Hz, Ar H-7), 4.04 (s, 2H, $ArCH_2N$), 3.50 (brs, 2H, H-2,6), 3.11 (brs, 2H, H-2,6), 3.02 (brs, 2H, H-3,5), 2.90 (s, 3H, NCH_3), 2.67 (brs, 2H, H-3,5), 2.30 (s, 3H, CH_3).

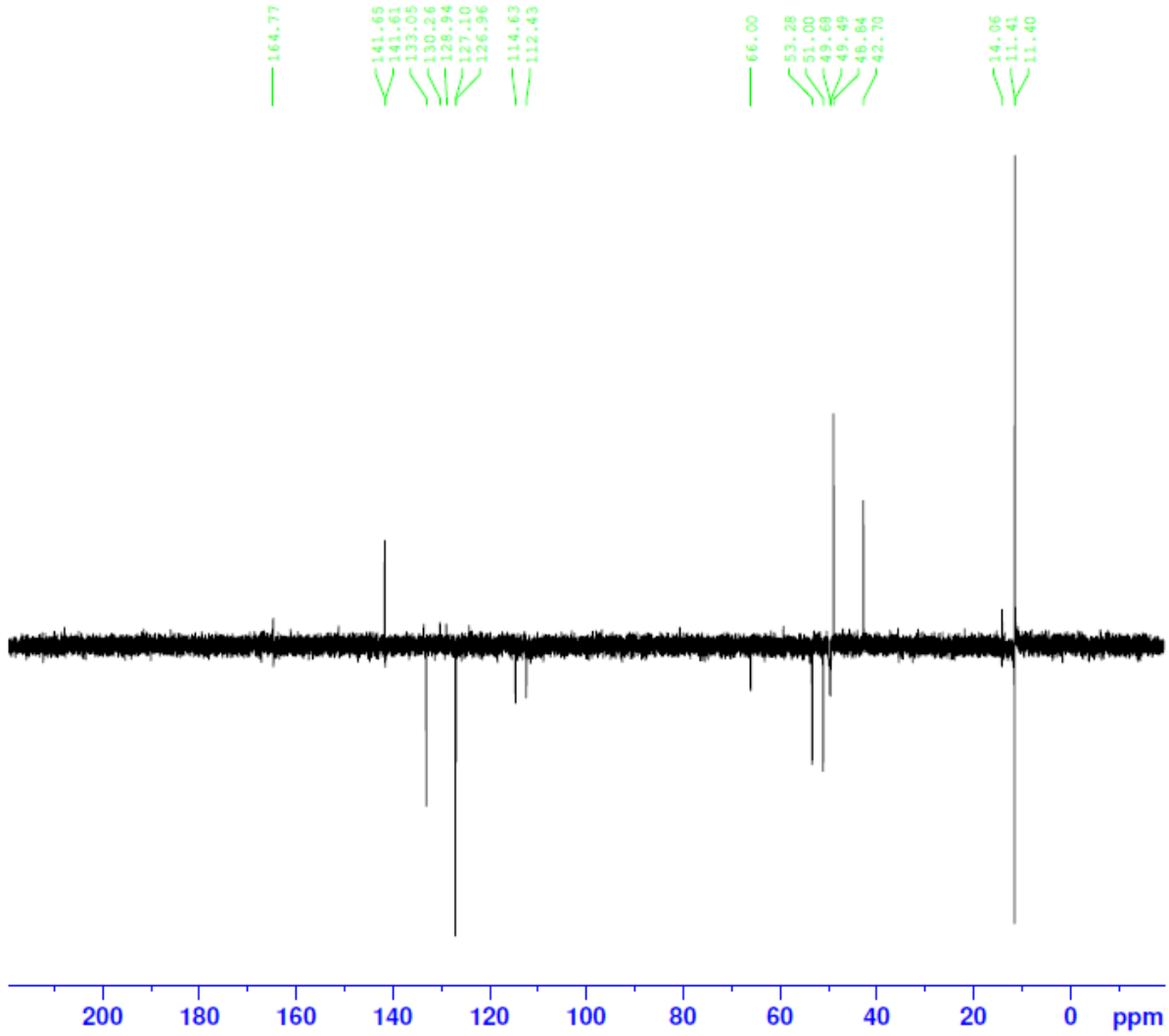

Figure 32: ^{13}C-NMR of the telenzepine rearrangement product measured with a resolution of 150 MHz in D_20.

^{13}C-NMR (150 MHz, D_2O) δ 164.9 (COOH), 151.2 (Ar C-2), 141.7 (thiophene C-4), 133.6 (Ar C-7a), 133.1 (thiophene C-2), 130.3 (Ar C-3a), 128.9 (thiophene C-3), 127.1 (Ar C-6), 127.0 (Ar C-5), 124.3 (thiophene C-5), 114.6 (Ar C-4), 112.4 (Ar C-7), 53.2 (C-2,6), 51.1 ($ArCH_2N$), 49.5 (C-3,5), 42.7 (NCH_3), 11.4 (CH_3).

5.4 Harvester experiments

Due to the inherent variance in biological systems all binding curves are shown as normalized graphs for a better comparison. In the chosen range of this experimental setup -12 represents the blank value (no competitor present) and -3 the unspecific binding of the tritiated scopolamine.

5.4.1 Pirenzepine

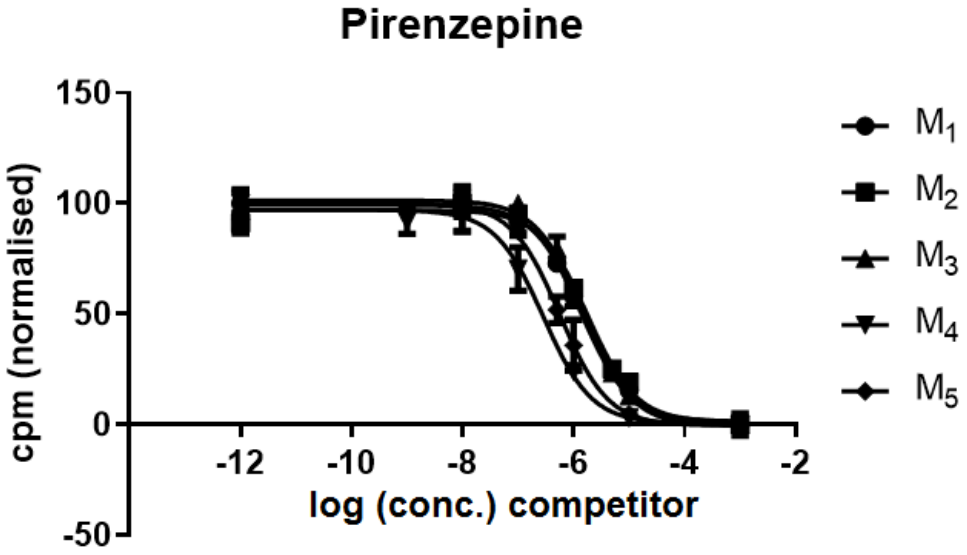

Figure 33: Normalized graph comparing all five mAChR subtype affinities of the binding assay for pirenzepine.

Table 19: Measured and calculated values of the competitive binding assay for pirenzepine and literature values from Valuskova et. al. for comparison.[14]

	M_1	M_2	M_3	M_4	M_5
IC_{50} [nM]	38	2761	1450	291	649
	23	1453	1201	186	446
	45	1794	1270	165	249
K_i value [nM]	18	1236	319	97	168
	11	650	264	62	116
	21	803	279	55	65
K_i mean [nM]	**17 ± 5**	**900 ± 300**	**290 ± 30**	**70 ± 20**	**120 ± 50**
Lit. K_i range [nM]	3 – 16	200 - 501	79 - 200	8 - 79	79 - 631

These results (fig. 33 and tab. 19) largely comply with the literature ranges from Valuskova *et al.* and also confirm that pirenzepine displays the highest affinity towards the M_1 mAChR subtype.[14]

5.4.2 Pirenzepine rearrangement product

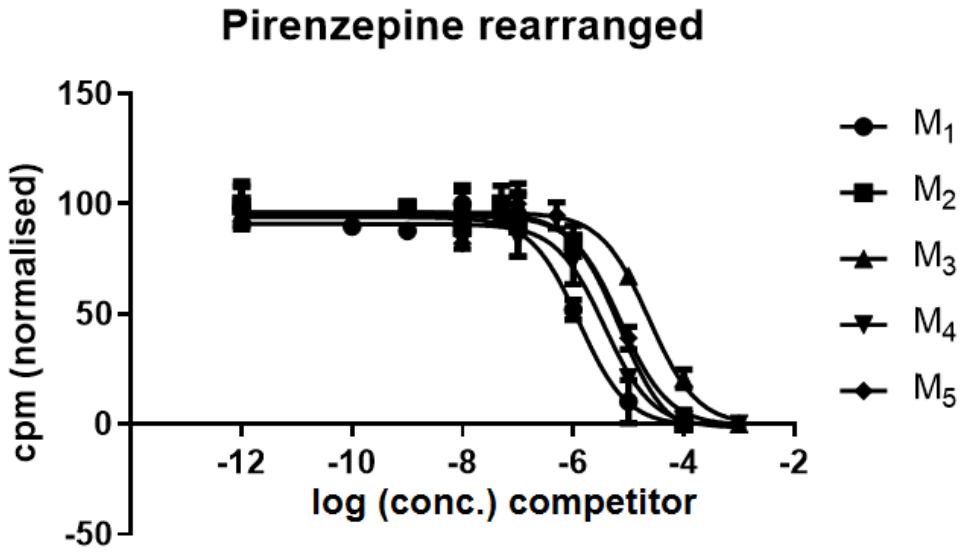

Figure 34: Normalized graph comparing all five mAChR subtype affinities of the binding assay for the pirenzepine rearrangement product.

Table 20: Measured and calculated values of the competitive binding assay for the pirenzepine rearrangement product (PR) and the K_i value range of pirenzepine (Pir.) from Valuskova et. al. for comparison.[14]

	M_1	M_2	M_3	M_4	M_5
IC_{50} [nM]	1330	151150	31200	4160	1310
	1240	93500	23600	2800	1420
	1250	70600	41300	3700	1450
K_i value [nM]	600	67640	6900	1400	300
	600	41800	5200	900	400
	600	31600	9100	1200	400
K_i PR mean [nM]	**600 ± 20**	**47000 ± 18600**	**7000 ± 1950**	**1190 ± 230**	**360 ± 20**
K_i Pir. range [nM]	3 – 16	200 - 501	79 - 200	8 - 79	79 - 631

The rearrangement product is three orders of magnitude less affine towards the muscarinic receptors (µM) compared to pirenzepine (fig. 34 and tab. 20). This decrease in affinity after the rearrangement comes as no surprise due to the complex nature of the receptor-ligand binding process which depends on the exact interaction of the components. However, the rearranged pirenzepine has structural similarities with drugs from a substance class called positive allosteric modulators (PAM) for the metabotropic glutamate receptors examined in Zhang *et al*. and Anderson *et al*.[51,52] PAMs can be separated into two types, ones that do not elicit biological responses on their own but after binding to the allosteric binding site, amplify the signal from the orthosteric binding site (pure PAM) and those which show agonistic properties when the natural ligand is not present as well as intensifying those responses (ago-PAM).[52] Therefore, the pirenzepine rearrangement product might serve as lead structure for designing new PAMs of the metabotropic glutamate receptors.

5.4.3 Telenzepine

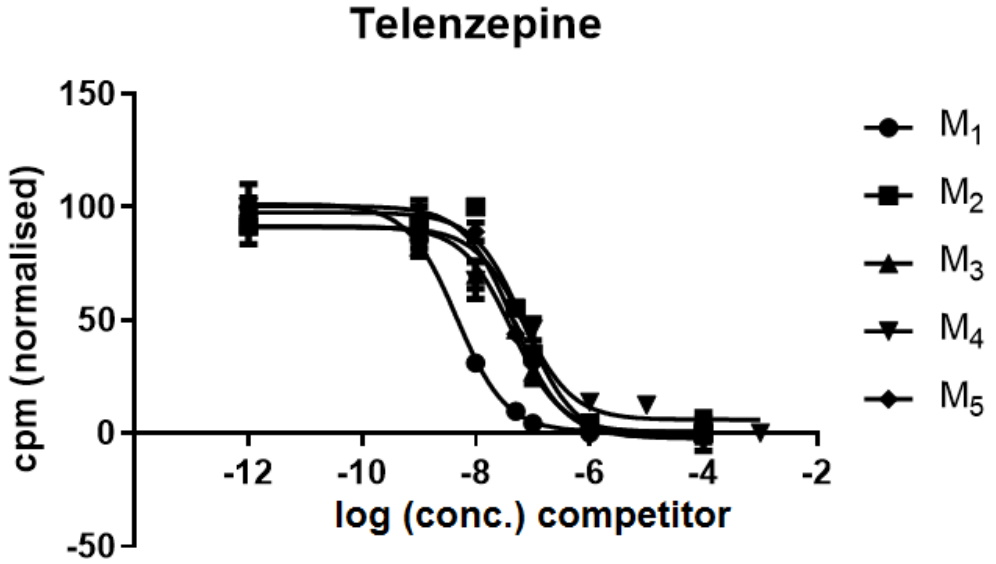

Figure 35: Normalized graphs comparing all five mAChR subtype affinities of the binding assay for telenzepine.

Table 21: Measured and calculated values of the competitive binding assay for telenzepine.

	M_1	M_2	M_3	M_4	M_5
IC_{50} [nM]	5	72	43	70	105
	2	49	57	143	46
	5	55	62	47	36
K_i value [nM]	3	32	9	23	27
	1	22	13	48	12
	2	24	14	16	9
K_i mean [nM]	**2 ± 1**	**26 ± 5**	**12 ± 2**	**30 ± 20**	**16 ± 10**

Table 22: Comparison of the subtype affinities of telenzepine with pirenzepine and literature values from Galvan et al.[21]

	M_1	M_2	M_3	M_4	M_5
Pirenzepine K_i [nM]	17 ± 5	900 ± 300	290 ± 30	70 ± 20	120 ± 50
Telenzepine K_i [nM]	2 ± 1	26 ± 5	12 ± 2	30 ± 20	16 ± 10
Literature Telenzepine K_i [nM]	0.94	17.8	N/A	N/A	N/A

Comparing the measured values (fig. 35 and tab. 22) to the telenzepine affinities for the M_1 and M_2 mAChR subtypes from Galvan *et al*. it can be seen that the results are in agreement with the literature and it could be also shown that telenzepine is four times more affine towards the M_1 subtype than pirenzepine (tab. 22).[20,21]

5.4.4 Telenzepine rearrangement product

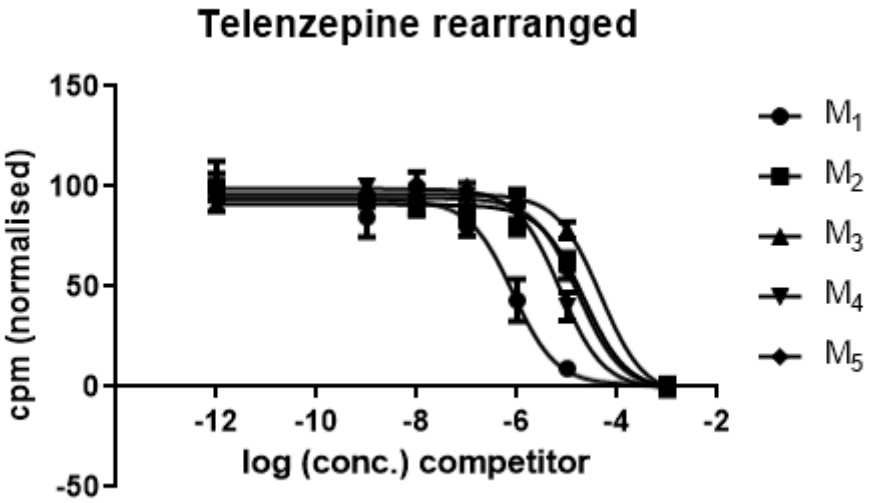

Figure 36: Normalized graph comparing all five mAChR subtype affinities of the binding assay for the telenzepine rearrangement product.

Table 23: Measured and calculated values of the competitive binding assay for the telenzepine rearrangement product.

	M_1	M_2	M_3	M_4	M_5
IC_{50} [nM]	2080	21300	22500	4760	15800
	3470	27310	46300	6110	14900
	3010	22120	41200	7200	16600
K_i value [nM]	1000	9500	4900	1600	4100
	1600	12200	10200	2000	3900
	1400	9900	9100	2400	4300
K_i mean [nM]	**1400 ± 340**	**10600 ± 1460**	**8100 ± 2750**	**2000 ± 410**	**4100 ± 220**

Due to the similar conditions of the rearrangement of telenzepine compared to pirenzepine, results were obtained that closely resemble those of the pirenzepine rearrangement product (fig. 36 and tab, 23). The yielded values are also in the order of three magnitude less affine towards the mAChR subtypes and the structure of the rearranged telenzepine has similarities with PAMs for the metabotropic glutamate receptors as well as described in Zhang *et al*. and Anderson *et al*.[51,52]

6 Conclusion and outlook

This master thesis could affirm the proposed reaction mechanism of the newly discovered acidic and quantitative rearrangement of pirenzepine through chemical kinetic studies and an analogous rearrangement reaction could be presented for the derivative telenzepine. This was achieved through the development of respective RP-HPLC gradient programs for each substance of interest, which assured a quick and reliable separation of the starting compound from its rearrangement product. The two literature unknown rearrangement products were characterized through UV spectroscopy, NMR, XRD and logP measurements. Further, regarding changes in their biological properties compared to their starting materials, competitive binding assays demonstrate that the rearrangement products exhibit a decrease in affinity of three orders of magnitudes towards all five mAChR subtypes, while K_i values for pirenzepine and telenzepine were adequately reproduced and logP measurements revealed a shift towards more hydrophilic characteristics for the rearrangement products. However, given the logP results there is a certain limitation to consider. The applied HPLC method was not optimal for the investigated compounds due to their hydrophilic properties being at the lower end or below of the effective range. Additionally, we could reaffirm the drug safety of pirenzepine, as the drug did not undergo the investigated rearrangement in simulated gastric fluid even after monitoring the reaction for 72 hours under physiological conditions and calculations of the kinetic studies yielded an estimated activation energy of 83.2 ± 1.9 kJ/mol necessary for the process to occur. Throughout the course of this master thesis a light could be shone on many aspects of the rearrangement reaction and its products, but more information needs to be acquired. Hence, follow-up experiments would include the crystallisation of AFDX-384 to confirm a similar rearrangement with subsequent chemical and biological characterization and an evaluation of the rearrangement products in terms of their potential application. Regarding the drug safety issue of pirenzepine, authorities in charge will be notified of the existence of the rearrangement product, so it can be included in literature as a possible contamination. Even a long-established drug such as pirenzepine potentially passed many quality assurance analyses with a by-product going unnoticed and therefore this work should be taken as yet another example to highlight the importance of proper chemical quality control. Finally, this master's thesis is a contribution to the dissertation of Marius Ozenil which elaborates on the discussed topics in further detail.

7 References

1. Tiwari P, Dwivedi S, Singh MP, Mishra R, Chandy A. Basic and modern concepts on cholinergic receptor: A review. *Asian Pacific J Trop Dis*. 2013;3(5):413-420. doi:10.1016/S2222-1808(13)60094-8

2. Brown DA. Acetylcholine and cholinergic receptors. *Brain Neurosci Adv*. 2019;3:239821281882050. doi:10.1177/2398212818820506

3. Jones CK, Byun N, Bubser M. Muscarinic and nicotinic acetylcholine receptor agonists and allosteric modulators for the treatment of schizophrenia. *Neuropsychopharmacology*. 2012;37(1):16-42. doi:10.1038/npp.2011.199

4. Aronstam RS, Patil P. Muscarinic Receptors: Autonomic Neurons. *Encycl Neurosci*. 2009:1141-1149. doi:10.1016/B978-008045046-9.00692-6

5. Ishii M, Kurachi Y. Muscarinic Acetylcholine Receptors. *Curr Pharm Des*. 2006;12(28):3573-3581. doi:10.2174/138161206778522056

6. Kruse AC, Kobilka BK, Gautam D, Sexton PM, Christopoulos A, Wess J. Muscarinic acetylcholine receptors: Novel opportunities for drug development. *Nat Rev Drug Discov*. 2014;13(7):549-560. doi:10.1038/nrd4295

7. Langmead CJ, Watson J, Reavill C. Muscarinic acetylcholine receptors as CNS drug targets. *Pharmacol Ther*. 2008;117(2):232-243. doi:10.1016/j.pharmthera.2007.09.009

8. Syha Y, Popescu L, Wurglics M, Schubert-Zsilavecz M. Ein historischer rückblick: Geschichte der ulcustherapie. *Pharm Unserer Zeit*. 2005;34(3):188-192. doi:10.1002/pauz.200500117

9. Carmine AA, Brogden RN. Pirenzepine: A Review of its Pharmacodynamic and Pharmacokinetic Properties and Therapeutic Efficacy in Peptic Ulcer Disease and Other Allied Diseases. *Drugs*. 1985;30(2):85-126. doi:10.2165/00003495-198530020-00001

10. Boehringer Ingelheim. Fachinformation Gastrozepin ® 50 mg. www.bfarm.de. Accessed June 29, 2020.

11. Pelat M, Lazartigues E, Tran MA, et al. Characterization of the central muscarinic cholinoceptors involved in the cholinergic pressor response in anesthetized dogs. *Eur J Pharmacol*. 1999;379(2-3):117-124. doi:10.1016/S0014-2999(99)00508-7

12. Tan DTH, Lam DS, Chua WH, Shu-Ping DF, Crockett RS. One-year multicenter, double-masked, placebo-controlled, parallel safety and efficacy study of 2% pirenzepine ophthalmic gel in children with myopia. *Ophthalmology*. 2005;112(1):84-91. doi:10.1016/j.ophtha.2004.06.038

13. Rahman Y, Afrin S, Tabish M. Interaction of pirenzepine with bovine serum albumin and effect of β-cyclodextrin on binding: A biophysical and molecular docking approach. *Arch Biochem Biophys*. 2018;652(June):27-37. doi:10.1016/j.abb.2018.06.005

14. Valuskova P, Farar V, Forczek S, Krizova I, Myslivecek J. Autoradiography of 3H-pirenzepine and 3H-AFDX-384 in mouse brain regions: Possible insights into M1, M2, and M4 muscarinic receptors distribution. *Front Pharmacol*. 2018;9(FEB):1-15. doi:10.3389/fphar.2018.00124

15. Martin J, Deagostino A, Perrio C, et al. Syntheses of R and S isomers of AF-DX 384, a selective antagonist of muscarinic M2 receptors. *Bioorganic Med Chem*. 2000;8(3):591-

600. doi:10.1016/S0968-0896(99)00307-7

16. Teaktong T, Piggott MA, Mckeith IG, Perry RH, Ballard CG, Perry EK. Muscarinic M2 and M4 receptors in anterior cingulate cortex: Relation to neuropsychiatric symptoms in dementia with Lewy bodies. *Behav Brain Res*. 2005;161(2):299-305. doi:10.1016/j.bbr.2005.02.019

17. Gibbons AS, Scarr E, McLean C, Sundram S, Dean B. Decreased muscarinic receptor binding in the frontal cortex of bipolar disorder and major depressive disorder subjects. *J Affect Disord*. 2009;116(3):184-191. doi:10.1016/j.jad.2008.11.015

18. Mickala P, Boutin H, Bellanger C, Chevalier C, MacKenzie ET, Dauphin F. In vivo binding, pharmacokinetics and metabolism of the selective M2 muscarinic antagonists [3H]AF-DX 116 and [3H]AF-DX 384 in the anesthetized rat. *Nucl Med Biol*. 1996;23(2):173-179. doi:10.1016/0969-8051(95)02015-2

19. Schudt C, Boer R, Eltze M, Riedel R, Grundler G, Birdsall NJM. The affinity, selectivity and biological activity of telenzepine enantiomers. *Eur J Pharmacol*. 1989;165(1):87-96. doi:10.1016/0014-2999(89)90773-5

20. Pediani JD, Ward RJ, Godin AG, Marsango S, Milligan G. Dynamic regulation of quaternary organization of the m1 muscarinic receptor by subtype-selective antagonist drugs. *J Biol Chem*. 2016;291(25):13132-13146. doi:10.1074/jbc.M115.712562

21. Galvan M, Boer R, Schudt C. Interaction of telenzepine with muscarinic receptors in mammalian sympathetic ganglia. *Eur J Pharmacol*. 1989;167(1):1-10. doi:10.1016/0014-2999(89)90741-3

22. Clayden J, Moran WJ, Edwards PJ, Laplante SR. The challenge of atropisomerism in drug discovery. *Angew Chemie - Int Ed*. 2009;48(35):6398-6401. doi:10.1002/anie.200901719

23. Londong W, Londong V, Meierl A, Voderholzer U. Telenzepine is at least 25 times more potent than pirenzepine - A dose response and comparative secretory study in man. *Gut*. 1987;28(7):888-895. doi:10.1136/gut.28.7.888

24. Eltze M, Gönne S, Riedel R, Schlotke B, Schudt C, Simon WA. Pharmacological evidence for selective inhibition of gastric acid secretion by telenzepine, a new antimuscarinic drug. *Eur J Pharmacol*. 1985;112(2):211-224. doi:10.1016/0014-2999(85)90498-4

25. Wedler G, Freund H-J. *Lehrbuch Der Physikalischen Chemie*. Sechste Ed. Wiley-VCH Verlag GmbH & Co. KGaA; 2012.

26. Atkins P, De Paula J. *Atkins' Physical Chemistry*. Ninth Edit. Oxford University Press; 2010.

27. Peleg M, Normand MD, Corradini MG. The Arrhenius equation revisited. *Crit Rev Food Sci Nutr*. 2012;52(9):830-851. doi:10.1080/10408398.2012.667460

28. Pollard TD. MBOC technical perspective: A guide to simple and informative binding assays. *Mol Biol Cell*. 2010;21(23):4061-4067. doi:10.1091/mbc.E10-08-0683

29. Davenport AP, Russell FD. Radioligand Binding Assays: Theory and Practice. In: *Current Directions in Radiopharmaceutical Research and Development*. Dordrecht: Springer Netherlands; 1996:169-179. doi:10.1007/978-94-009-1768-2_11

30. Motulsky H, Neubig R. Analyzing Radioligand Binding Data. *Curr Protoc Neurosci*. 2002;19(1):1-55. doi:10.1002/0471142301.ns0705s19

31. Yung-Chi C, Prusoff WH. Relationship between the inhibition constant (KI) and the concentration of inhibitor which causes 50 per cent inhibition (I50) of an enzymatic reaction. *Biochem Pharmacol*. 1973;22(23):3099-3108. doi:10.1016/0006-2952(73)90196-2

32. Qume M. Overview of ligand-receptor binding techniques. *Methods Mol Biol*. 1999;106:3-23. doi:10.1385/0-89603-530-1:3

33. Merck KGaA. Protease Inhibitor Cocktail for general cell lysate enzyme inhibition. | Sigma-Aldrich. https://www.sigmaaldrich.com/catalog/product/sigma/p2714?lang=de&region=AT. Accessed July 23, 2020.

34. Wei GX, Bobek LA. Human salivary mucin MUC7 12-mer-L and 12-mer-D peptides: Antifungal activity in saliva, enhancement of activity with protease inhibitor cocktail or EDTA, and cytotoxicity to human cells. *Antimicrob Agents Chemother*. 2005;49(6):2336-2342. doi:10.1128/AAC.49.6.2336-2342.2005

35. Tocris Bioscience. AF-DX 384 Supplier | CAS 118290-26-9 | Tocris Bioscience. https://www.tocris.com/products/af-dx-384_1345. Accessed November 11, 2019.

36. Sturm E, Junker A. Determination of telenzepine in human serum by gas chromatography-mass spectrometry. *J Chromatogr B Biomed Sci Appl*. 1988;430(C):43-51. doi:10.1016/S0378-4347(00)83132-1

37. European Medicines Agency. ICH Topic Q 2 (R1) Validation of Analytical Procedures: Text and Methodology. In: ; 1994.

38. Donovan SF, Pescatore MC. Method for measuring the logarithm of the octanol-water partition coefficient by using short octadecyl-poly(vinyl alcohol) high-performance liquid chromatography columns. *J Chromatogr A*. 2002;952(1-2):47-61. doi:10.1016/S0021-9673(02)00064-X

39. Vraka C, Nics L, Wagner KH, Hacker M, Wadsak W, Mitterhauser M. LogP, a yesterday's value? *Nucl Med Biol*. 2017;50:1-10. doi:10.1016/j.nucmedbio.2017.03.003

40. Muszyńska B, Krakowska A, Lazur J, et al. Bioaccessibility of phenolic compounds, lutein, and bioelements of preparations containing Chlorella vulgaris in artificial digestive juices. *J Appl Phycol*. 2018;30(3):1629-1640. doi:10.1007/s10811-017-1357-2

41. Spingler B, Schnidrig S, Todorova T, Wild F. Some thoughts about the single crystal growth of small molecules. *CrystEngComm*. 2012;14(3):751-757. doi:10.1039/c1ce05624g

42. Hoffmann C, Leitz MR, Oberdorf-Maass S, Lohse MJ, Klotz KN. Comparative pharmacology of human β-adrenergic receptor subtypes - Characterization of stably transfected receptors in CHO cells. *Naunyn Schmiedebergs Arch Pharmacol*. 2004;369(2):151-159. doi:10.1007/s00210-003-0860-y

43. drugbank.ca. Pirenzepine - DrugBank. https://www.drugbank.ca/drugs/DB00670. Accessed November 3, 2019.

44. guidetopharmacology.org. AFDX384 | Ligand page | IUPHAR/BPS Guide to

PHARMACOLOGY. https://www.guidetopharmacology.org/GRAC/LigandDisplayForward?tab=biology&ligandId=3264. Accessed November 3, 2019.

45. chemspider.com. Telenzepine | C19H22N4O2S | ChemSpider. http://www.chemspider.com/Chemical-Structure.5194.html. Accessed November 3, 2019.

46. Arnott JA, Planey SL. The influence of lipophilicity in drug discovery and design. *Expert Opin Drug Discov*. 2012;7(10):863-875. doi:10.1517/17460441.2012.714363

47. OECD. *Test No. 117: Partition Coefficient (n-Octanol/Water), HPLC Method*. OECD; 2004. doi:10.1787/9789264069824-en

48. Cox AJ. Variations in Size of the Human Stomach. *Cal West Med*. 1945;63(6):267-268. http://www.ncbi.nlm.nih.gov/pubmed/18747178.

49. Fruton JS. 4 Pepsin. In: ; 1971:119-164. doi:10.1016/S1874-6047(08)60395-9

50. Schanker LS. Absorption of Drugs from the Gastrointestinal Tract. In: Brodie BB, Gillette JR, Ackerman HS, eds. *Concepts in Biochemical Pharmacology: Part 1*. Berlin, Heidelberg: Springer Berlin Heidelberg; 1971:9-24. doi:10.1007/978-3-642-65052-9_2

51. Zhang L, Brodney MA, Candler J, et al. 1-[(1-methyl-1 H-imidazol-2-yl)methyl]-4-phenylpiperidines as mGluR2 positive allosteric modulators for the treatment of psychosis. *J Med Chem*. 2011;54(6):1724-1739. doi:10.1021/jm101414h

52. Anderson PS, Bernstein PR, Brown SP, et al. *Annual Reports in Medical Chemistry*. Volume 47. (Manoj C. Desai, ed.). Elsevier B.V.; 2012.

Table of figures

Table of tables

Table of equations